CCD TRANSFORMATION EQUATIONS FOR USE WITH SINGLE-IMAGE PHOTOMETRY

Bruce L. Gary (GBL)
Hereford, AZ

March 2006

Note: This document is an expanded version of a shorter document ([CCD Transformation Equations](#)) that is linked to by the AAVSO ([AAVSO CCD Observing Manual](#)). That document is confined to a description of the traditional use of "CCD Transformation Equations." This document repeats the AAVSO linked version, but has an added section at the end where I describe an alternative to the traditional calibration methodology which I believe to be easier to use and possibly more accurate. Anyone who has read the other document will want to skip down to the last section of this document for the new material, at [Alternative Calibration Procedure](#). The material ahead of this section is referred to in the last section, and since it provides necessary context it is included in this document.

Abstract

CCD photometry requires that corrections be made for a specific user's unique spectral response for blue, visible, red and infra-red filters. A system's calibration is unique principally due to filter pass band characteristics, the telescope's spectral response, the CCD's spectral response and also atmospheric extinction properties that depend on elevation angle in a way that changes with time. The "CCD Transformation Equations" are intended to remove most of these effects, allowing for the combining of multi-color photometric observations made by many observers.

The specific set of equations to be used depends on which of several possible filter combinations are used. Whenever at least two filters are employed, such as BV, VR or RI, transformation equation corrections can be applied. The most common set in use is the three color combination BVR. For this filter set the following transformation equations are to be used:

$(V_s - R_s) = (V_c - R_c) + T_{vr} * [(v_s - r_s) - (v_c - r_c)]$

$V_s = v_s + (V_c - v_c) + T_v * [(V_s - R_s) - (V_c - R_c)]$, *using the solution for $(V_s - R_s)$ in the above line*

$R_s = V_s - (V_s - R_s)$, *using V_s from the line above, and $(V_s - R_s)$ from the first line*

$B_s = V_s + (B_c - V_c) + T_{bv} * [(b_s - v_s) - (b_c - v_c)]$

assuming the following coefficient definitions:

Tv = *slope of (V-v) plotted versus (V-R)*

Tvr = *reciprocal of slope of (v-r) plotted versus (V-R)*

Tbv = *reciprocal of slope of (b-v) plotted versus (B-V)*

This document describes the derivation of this equation, as well as the equations that are to be used for all other filter combinations. Examples are given for deriving the coefficients, and reducing observations with the BVR set. An alternative procedure for correcting multi-color photometric observations is described in the last section of this document. Although this alternative procedure is much simpler, it should be used with the knowledge that it is not an accepted standard. Until it is shown to be reliable it should only be used for "checking" suspect results using the AAVSO-sanctioned CCD Transformation Equation results.

I. Introduction.

This document is meant for new CCD observers wishing to make photometric quality measurements of the magnitude of stellar objects using BVRI filters.

When I started doing this it was difficult to locate information on the Internet or in books for amateur astronomers that explained the procedure for correcting color filter observations for errors caused by slight differences between an observer's "system spectral response" for each filter and a reference standard spectral response. A commonly used correction procedure makes use of "CCD Transformation Equations" which require that each observer determine **coefficients** used by the transformation equations. Each observing system has a unique set of coefficient values, and these values should be determined about once per year to monitor any changes in filter or CCD properties. The purpose of this document is to provide a simple explanation of the procedure for determining the transformation equation coefficients, the procedure for using the transformation equations to correct a set of observations, and the rationale for this entire procedure.

The AAVSO (American Association of Variable Star Observers) has a document explaining the use of CCDs for photometry, and it also contains a description of CCD Transformation Equations. This is a great starting place for any observer wanting to understand how to perform quality CCD photometry for submission to the AAVSO. That page is at AAVSO CCD Photometry Manual. (http://www.aavso.org/ccd/manual/)

II. The Reasons Magnitude Corrections Are Necessary

This section illustrates the way typical differences in filters spectral response and CCD spectral response contribute to errors in the measurements of star magnitudes. It makes the case for the practice of performing CCD transformation equation corrections before submission to AASVO. The following sections show how to make those corrections.

In order to compare observations of the brightness of a given object made by different observers it is necessary to correct for differences in the spectral response of each observer's system and observing situation. The term "observer's system" refers to the CCD, filters, and telescope. The term "observing situation" refers to the atmosphere through which the observations are made. Both the hardware and the atmosphere can affect the spectral response associated with an observation using a specific filter.

The concept of "spectral response" is important throughout all that is dealt with here, so let's deal with that first. Consider a single observation (or integration) of a field of interest using a single filter. The term "spectral response" refers to the probability that photons of light having different energies (wavelengths) will successfully pass through the atmosphere (without being scattered or absorbed) and pass through the telescope and filter and then be registered by the CCD at some pixel location. This probability versus wavelength, called spectral response, varies with photon wavelength, ranging from zero at all short wavelengths, to maybe 20% (as described below) near the center of the filter's response function, and back to zero for all longer wavelengths. The spectral response will be a smooth function, having steep slopes on both the short-wavelength cut-on and long wavelength cut-off sides of the response function. The entire journey of a photon through the atmosphere, the telescope, the filter, and it's interaction with

the CCD chip, where it hopefully will dislodge an electron that will later be collected by the CCD electronics when the integration has finished, can be summarized by "probability versus wavelength" functions, described next.

Atmospheric Absorption and Scattering

The first obstacle on a photon's journey to the observer's image file is the atmosphere.
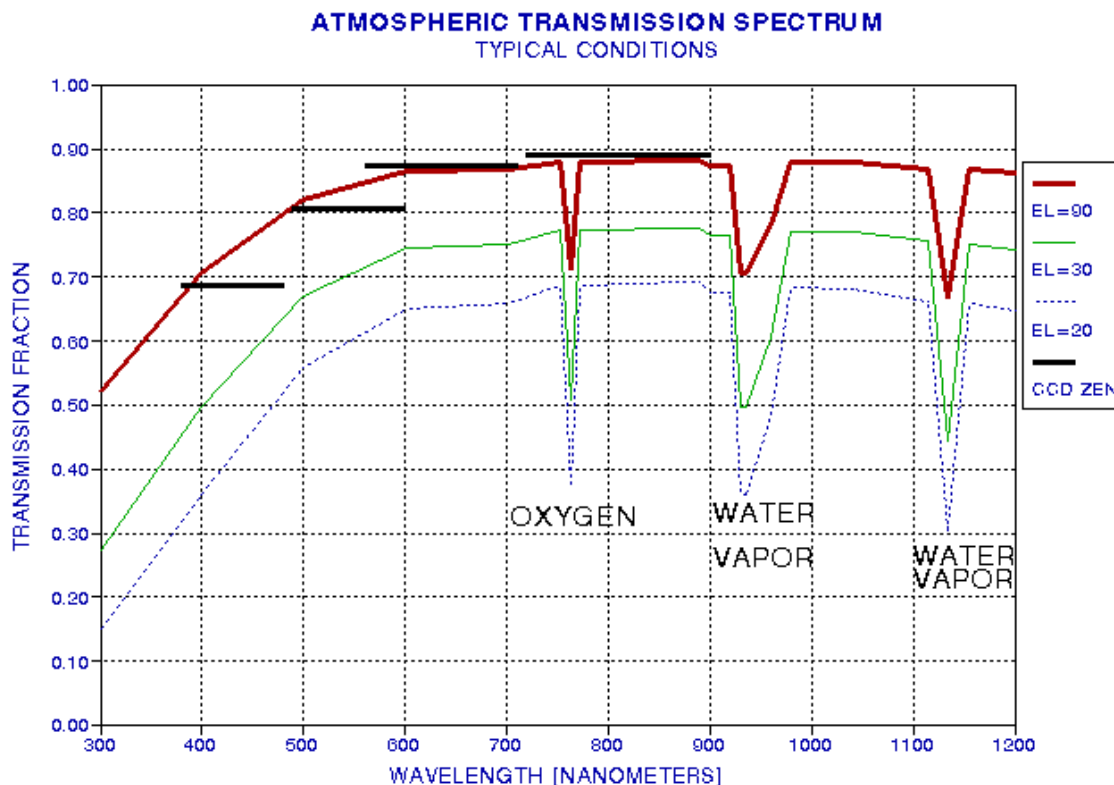
Figure 1 - Atmospheric transmission versus wavelength for typical conditions (water vapor burden of 2 cm, few aerosols), for three elevation angles (based on measurements by the author in 1990, at JPL, Pasadena, CA). Three absorption features are evident: a narrow feature at 763 nm, caused by oxygen molecules, and regions at 930 and 1135 nm caused by water vapor molecules. Four thick black horizontal lines show zenith transparency based on measurements made (by the author) with a CCD/filter wheel/telescope for typical clear sky conditions on another date and at another location (2002.04.29, Santa Barbara, CA, SBIG ST-8E, Schuler filters B, V, R and I).

This figure can be used to state, for example, that photons of wavelength 500 nm (nanometers) coming in from a 30 degree elevation angle have a 67% probability of reaching the ground. The same photons coming from lower elevation angles have a lower probability of reaching the ground. Due to absorption by water vapor molecules, at 940 nm the probability of photons reaching the ground is only about 40% for the 20 degree elevation angle path. During cloudless conditions most photons make it to ground level without being absorbed or scattered.

The depths of the three absorption "features" are not the same for all observers. For example, the 763 nm oxygen feature is altitude dependent, being about 60% of its surface value at Mauna Kea's altitude (13,800 feet). For most amateurs this feature can be disregarded since it is has such a narrow spectral

width and its site dependence is small. Within the two water vapor absorption regions, however, changes in absorption can be dramatic. The number of water vapor molecules per unit volume decreases rapidly with altitude. At upwind coastal sites (such as California's west coast) most of the overhead water vapor is confined to the lowest 2000 feet; and above this marine "planetary boundary layer" is dry continental air, with quite small overhead water vapor contents. A sea level site may have twice the overhead water vapor "burden" as a site at the top of a 2000-foot coastal mountain range. At Mauna Kea, for example, the water vapor absorption features will be miniscule (I once measured a value that was a mere 3% of a corresponding sea level value). Water vapor burdens vary with season at mid-latitudes (about 3 to 1) but do not vary with season in the tropics (where average water vapor burdens are three times greater than at mid-latitudes). At mid-latitudes there can be 2 to 1 variations from week to week, due to weather systems moving through. The absorption spectrum in Fig. 1 is just a guide to what's happening to photons on their journey to ground level.

Filter Pass Bands
Assuming the observer is using a reflector telescope, or a Schmidt-Cassegrain with small losses in the front glass corrector, the photon that makes it to ground level has a lossless path through the telescope to the filter. For observers using a refractor telescope, there may be losses in the objective lens due to reflections and absorptions. For a good objective, though, these losses will be small. The remainder of this section deals with what happens to ground-level photons that reach the filter.

There are two commonly used UBVRI filter response "standards" in use, going by the names Cousins/Bessell and Johnson. Most amateurs use filters adhering to the Johnson response shape. The two systems are essentially the same for UBV, and differ slightly for the R and I filter. Observations made with one filter type can be converted to the other using the CCD transformation equations, so it would be wrong to say that one is better than the other. The choice of one system over the other is less important than a proper use of either one (as Optec forcefully states on their document). Even filters from different manufacturers differ slightly from each other. The following figure shows a typical filter response for BVRI filters made by Schuler.
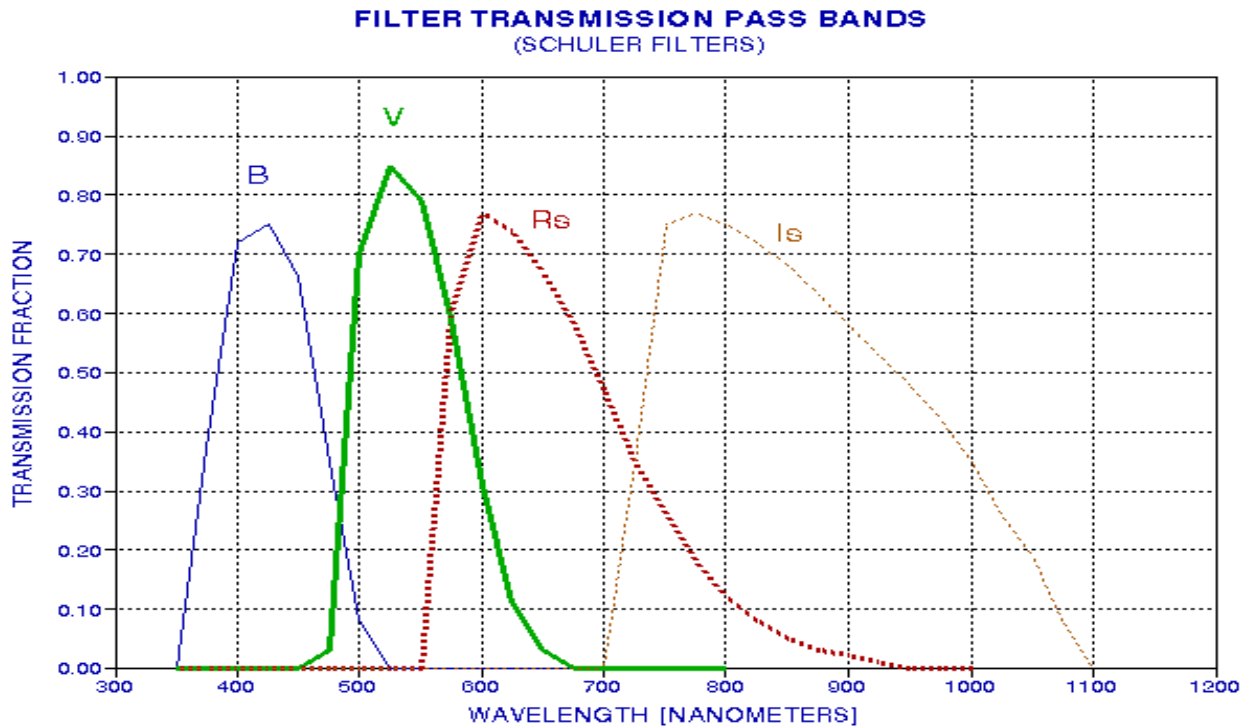
FILTER TRANSMISSION PASS BANDS
(SCHULER FILTERS)

Figure 2 - Typical BVRI filter spectral response (i.e., band pass)

Considering those 500 nm photons coming in from a 30 degree elevation, for which only 67% make it to ground level, they may have another 70% probability of passing through the V-filter, for example. In other words, only 47% of photons at the top of the atmosphere and coming in at a 30 degree elevation angle make it to the surface of the CCD chip.

CCD Chip Quantum Efficiency

Photons that make it through the atmosphere and filter still must reach the CCD chip if they are to register with the observer's image. There's a matter of cover plates, protecting the chip and preventing water vapor condensation, which is a minor obstacle for a photon's journey. The real challenge for photons is to deposit its energy within a pixel part of the CCD chip and dislodge an electron, setting it free to roam where it can be collected and later produce a voltage associated with the totality of electrons collected at that pixel location. The fraction of photons incident upon the CCD that can produce electrons in a collection "well" is the CCD's quantum efficiency. The quantum efficiency versus wavelength for a commonly used CCD chip is shown in the next figure.

CCD QUANTUM EFFICIENCY
(KAF 1602E, used in SBIG ST-8E)
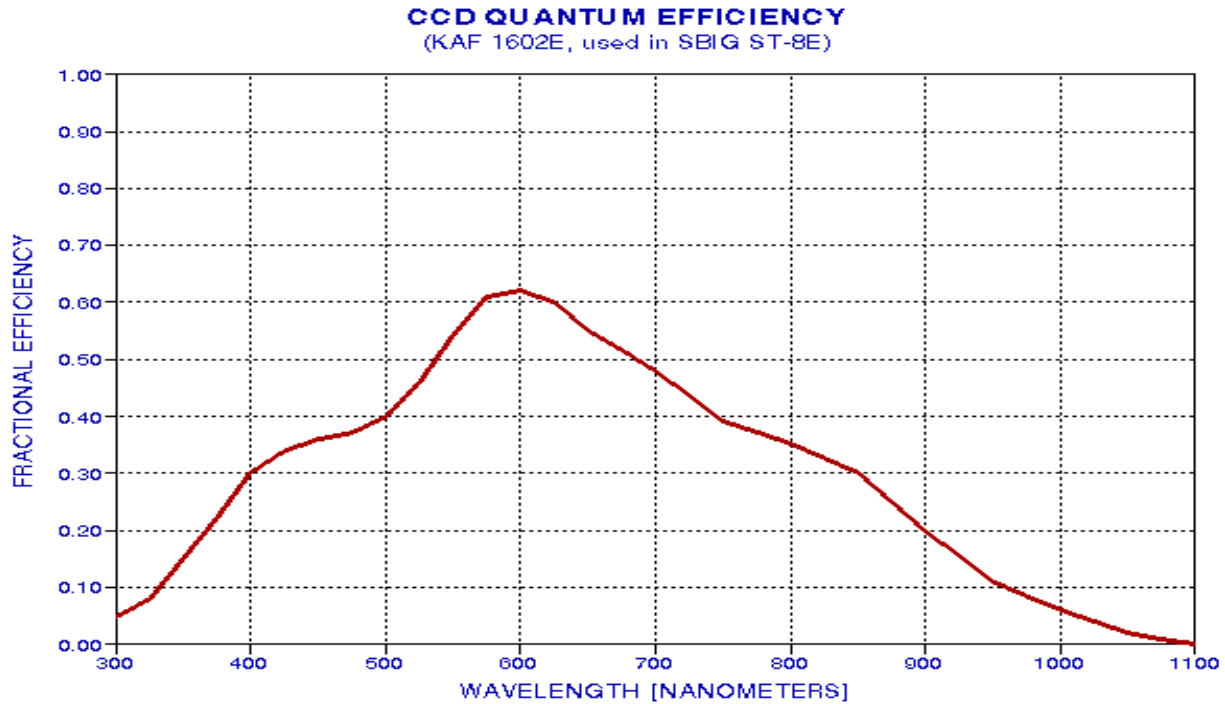
Figure 3 - Fraction of photons incident upon chip that free electrons for later collection
(KAF 1602E chip, used in the popular SBIG ST-8E CCD imager)

Considering again 500 nm photons, of those that reach a typical CCD chip, such as the one used in SBIG's ST-8E, only 40% dislodge an electron for later collection and measurement. For the V-filter, therefore, only 19% of those photons at the top of the atmosphere, coming in at 30 degrees elevation angle, actually get "counted" during an integration under typical clear weather conditions. This number is the product of three transmission functions given in the above three figures. Each filter has associated with it a total transmission probability, and it depends upon not only the filter characteristics, but also upon the atmosphere and the CCD properties. For the system used in this example, the following figure shows the spectral response for photons arriving at a 30 degree elevation angle, under typical weather conditions, going through Schuler filters and being detected by the KAF 1602E CCD chip.

Spectral Response Due to All Sources of Photon Loss

The following figure shows the fraction of photons starting at the top of the atmosphere that can be expected to contribute to a star's image for a typical atmosphere conditions, using typical filters and a commonly used CCD.
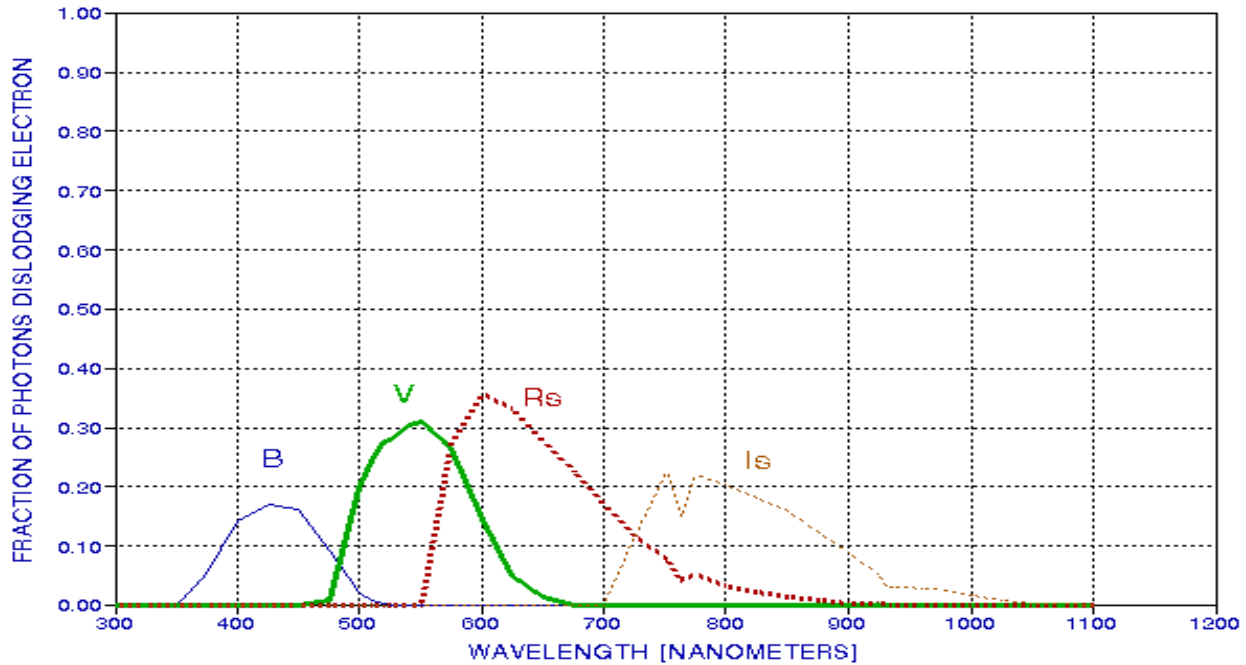
*Figure 4 - Response of entire "atmosphere/filter/CCD system" for typical water vapor burden,
few aerosols, 30 degree elevation angle, Schuler filters and SBIG ST-8E CCD (KAF 1602E chip)*

The reader may now understand how it happens that different observers can have different system spectral responses for their specific systems and atmospheric conditions. Two observers may be making measurements at the same time from different locations and using different filters and CCD imagers, and unless care is taken to convert their measurements to a "standard system" their reported magnitudes would differ. The magnitude differences will depend upon the "color" of the star under observation, as described in the next section.

Different Observers Have Different Pass Bands

To illustrate the fact that different observers can have different pass bands when they're both making B-filter measurements, let's consider two observers working side-by-side but using different filters and CCD. For example, before I purchased a SBIG ST-8E with Schuler filters, I used a Meade 416XTE CCD with their RGB filter set. The Meade B filter was intended for RGB color image creation, not for photometry. Since the filters weren't designed for photometry (as Meade acknowledges) they will require large corrections during the process of converting observations made with them to a standard system. For the purpose of this discussion, illustrating the concepts of filter differences, the Meade 616 filters provide are suitable example of the need to be careful. The next figure shows the "atmosphere/B-filter/CCD" spectral responses for the two systems under consideration.
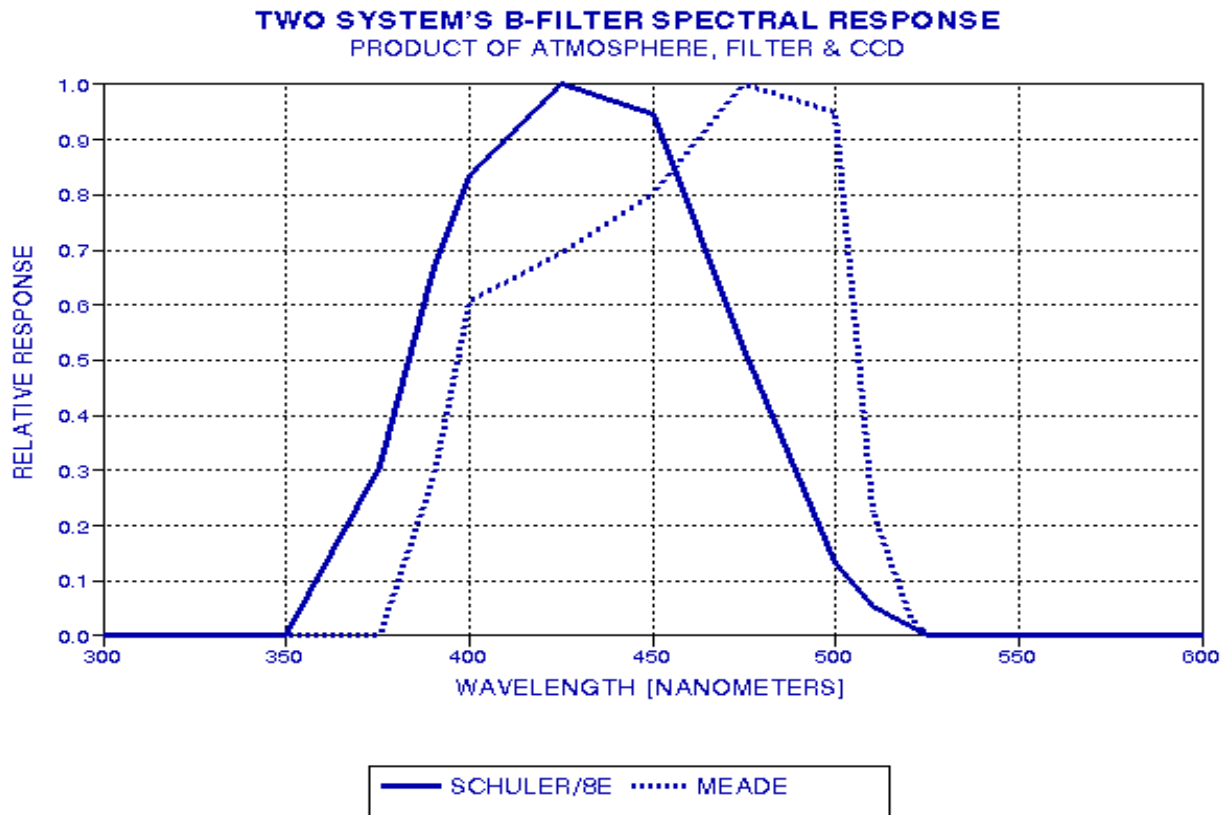
Figure 5 - Spectral response of different systems. The solid trace consists of a Schuler Bu filter, intended for photometry, and a SBIG ST-8E CCD, whereas the dotted trace is for a Meade B-filter and 416XTE CCD. The response for both systems corresponds to observing at an elevation angle of 30 degrees in a typical, clean atmosphere (2 cm precipitable water vapor). Both response traces are normalized to one at their peak response wavelength.

The Meade system has a spectral response that is shifted to longer wavelengths compared to the Schuler/SBIG ST-8E system. This shift may not seem like much, but consider how important it can be when observing stars with a spectral output that usually is falling off at shorter wavelengths throughout the wavelength region of these filter pass bands. The next figure shows a typical star's brightness versus wavelength.

B-FILTER RESPONSES & STELLAR SPECTRUM
(SPECTRUM OF STAR 'DENEB')

SCHULER/8E ⋯⋯ MEADE ── 4800 K STAR
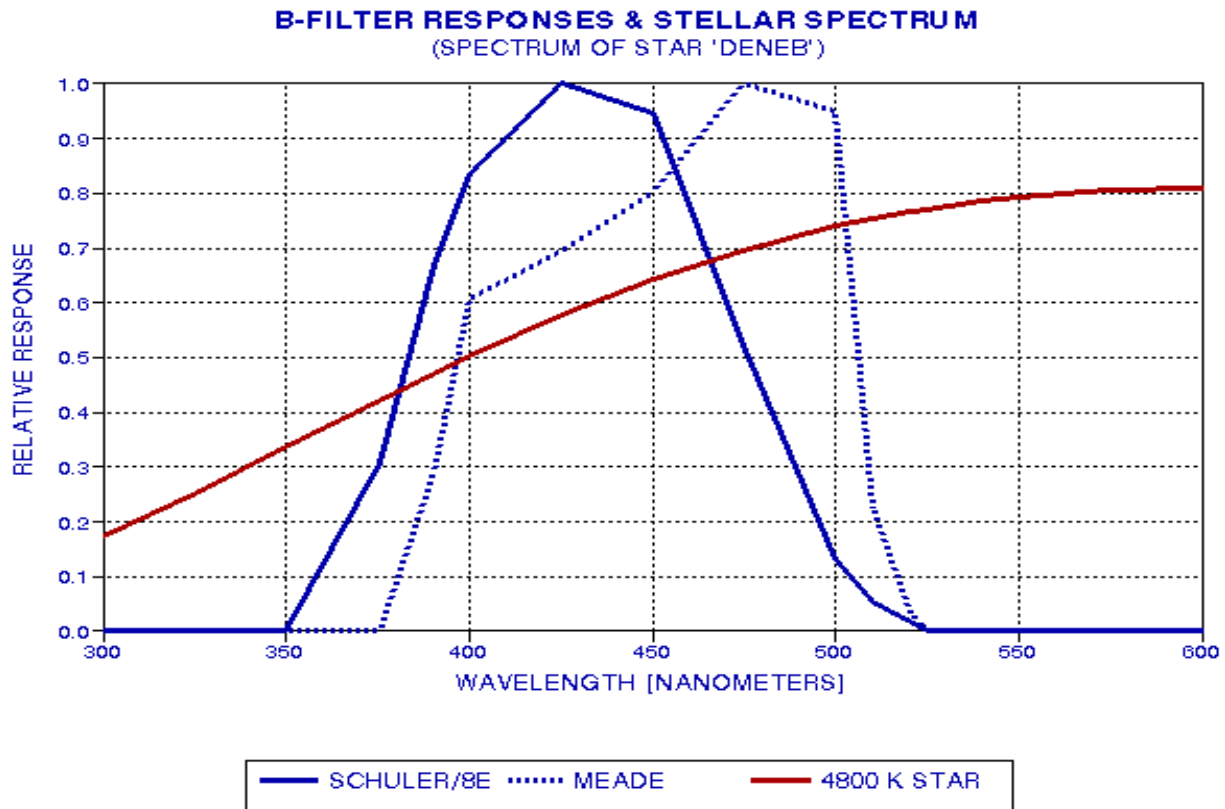
Figure 6 - Spectrum of a typical star, Deneb, having a surface temperature of 4800 K,
in relation to the two system's B-filter spectral responses.

When a typical star (such as Deneb, shown in the figure) is observed by both systems, the Meade system is observing "higher up" on the stellar brightness curve, producing a greater spectrum-integrated convolved response than for the Schuler/8E system. (The "spectrum-integrated convolved response" is the area under the curve of the product of the stellar source function with the filter response function.) For example, the ratio of spectrum-integrated convolved responses in this example is 1.137, corresponding to a magnitude difference of 0.14. In other words, the Meade system will measure a blue magnitude for Deneb that is too bright by 0.14 magnitudes, and whatever correction algorithm is used should end up adding approximately 0.14 magnitudes to the Meade system's B-magnitude. Redder stars will require greater corrections, and bluer stars will require smaller corrections.

Corrections of this amount are important, which illustrates the need for going to the trouble of performing CCD transformation equation corrections. Observers using filters intended for photometry use will presumably require smaller corrections than the 0.14 magnitudes of the example cited here. Since it is reasonable to try to achieve 0.03 magnitude accuracy, corrections for filter and CCD differences are an important part of the calibration process.

To the extent that the atmosphere can change the spectral response of an observer's atmosphere/filter/CCD for any of the BVRI configurations, it may be necessary to somehow incorporate "atmospheric extinction effects" into the data analysis procedure in order to assure that magnitude estimates are high quality. For example, Rayleigh scattering grows as the inverse 4th power of wavelength, so high air mass observations will shift the short wavelength cut-on of the blue filter more

than the same filter's long-wavelength cut-off. In effect, high air mass observations are being made with a blue filter that is shifted to the red. The effect of this will be greater for red stars than blue stars. A simple method is described below for performing a first order correction for atmospheric extinction effects.

III. Derivation of CCD Transformation Correction Equations - 4 Color Examples

The remainder of this document pertains to observers who will do "single image photometry." For the observer interested in "all sky photometry" I would like to suggest that you read through the All Sky Photometry Tutorial, http://brucegary.net/AllSky/x.htm , as well as other documents, articles, and books, and then decide if the "all sky" version is worth a try. Until then, feel a warm welcome to the forgiving world of "single image photometry" - and read on.

The following derivation is built up from simple cases, starting with approximations that illustrate the underlying concepts. Rigorous refinements are applied where needed.

The previous section should have convinced the reader that errors due to filter/CCD differences will vary with a star's "color." Hot stars are blue, cold stars are red. This just means that the "blackbody" distribution of radiant energy varies with wavelength differently, such that the slope of brightness versus wavelength across the region covered by a pair of filters is different for different stars. Comparison stars will have different temperatures, and hence they will have different spectral slopes for any pair of filters under consideration. The target object, such as a supernova, will certainly have a different spectral shape than the comparisons stars (being much redder, usually).

To begin, let's consider 2-color photometry, using R and I filters (red and infra-red). Later, we'll generalize this to the rest of the filter combinations.

Deriving Something Called T_{ri}

Given that errors in measured magnitude can be expected to correlate with star color, it is natural to wonder about the shape of scatter diagrams that will show this color dependence of measured magnitudes. Consider the case where a field of stars with known magnitudes is observed in a single CCD image. Measured R and I magnitudes are referred to as "r" and "i" whereas known magnitudes are referred to as "R" and "I". Two scatter plots will be found useful: 1) "R-I" versus "r-i" and 2) "R-r" versus "R-I". This is illustrated in the following figures.
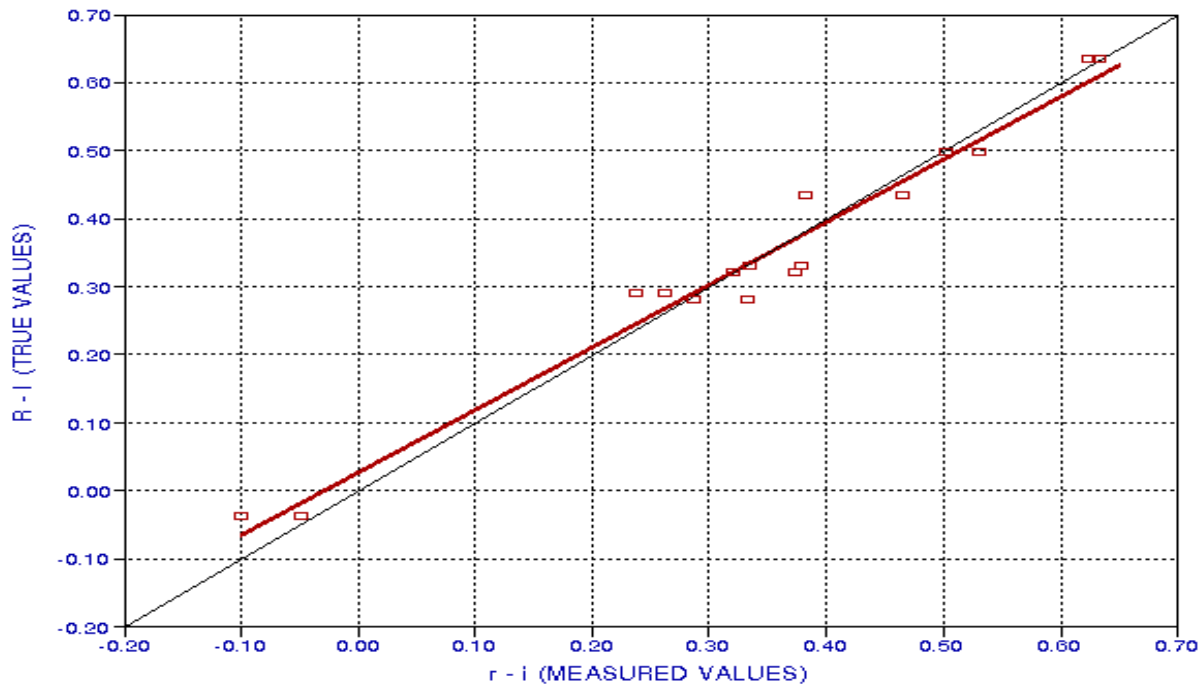
Figure 7 - Actual data (SBIG ST-8E and Schuler filters) for standard comparison stars in M67, showing a plot of known "R-I" versus measured "r-i." (Note: This scatter diagram is not a version that is used in deriving CCD transformation equation coefficients; it is presented here simply to illustrate a concept.)

The scatter plot in Fig. 7 illustrates that there appears to be a linear relation between true and measured star color "red minus infra-red". Consider this linear relation to be described by the following equation:

$$R\text{-}I = C_0 + C_1 * (r\text{-}i) \tag{Eqn. 1}$$

In other words, from an analysis of measured red and infra-red magnitudes of a set of standard stars it appears possible to convert any measured r-i star color to a corrected R-I star color. All that's needed are the two coefficients C_0 and C_1 in order to make the conversion. For example, if an object of interest, a supernova say, has a measured r-i of +0.10, then it seems safe to conclude that it has a true R-I of +0.12 (just by simply reading a Y-axis value off the fitted line at the X-axis value of +0.10).

Notice that we're using r and i magnitudes that haven't been calibrated yet. At this stage of analysis, the measured r and i magnitudes can have any calibration **offset** imaginable, and the procedure for determining a "corrected" R-I will not be affected.

The above description is just a small first step in understanding the concepts underlying CCD transformation equations. Before proceeding further, let's back-up a little and modify what we've done to conform with a fundamental principle pertaining to the handling of measurements. Notice that the scatter plot in Fig. 7 has measured values plotted as the abscissa (X-axis) and the true values as the ordinate (Y-axis). If error bars were used they'd be horizontal, which is kind of unusual. It's unusual because whenever measured values are "fitted" they must be treated as the dependent variable, reserving the true values as the independent variable. It is customary to represent this relationship by plotting measured quantities along the Y-axis versus known quantities along the X-axis. Thus, when we perform a least

squares "fit" (LS fit) to the measured quantities versus the known quantities, we're assuming that only the data point's Y-location is uncertain, and its X-location is known. Therefore, to prevent confusion over how the least squares solution is to be performed, we should plot the data of Fig. 7 with X-axis and Y-axis reversed, as in the following figure.
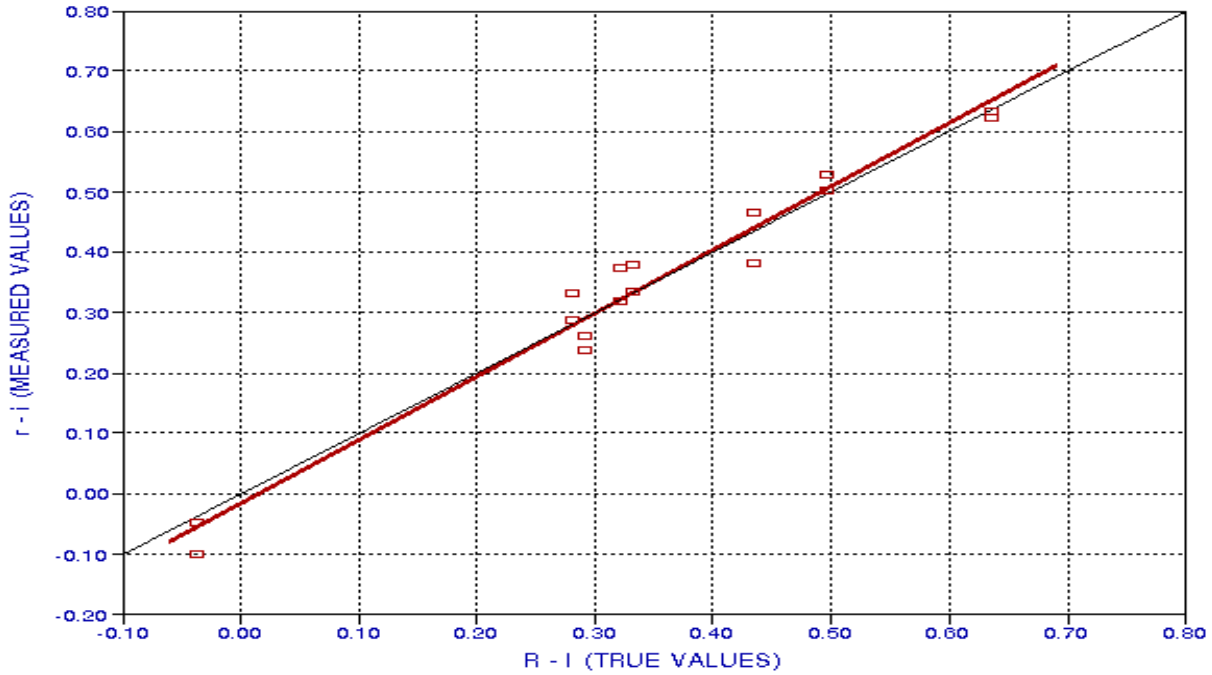

Figure 8 - Plot of measured "r - i" versus known "R - I" for a field of comparison stars (in M67). This is a proper way to display the data of the previous figure that conveys the fact that the least squares fit is to be performed with the measured "r-i" values as the dependent variable and known "R-I" values as the independent variable. The reciprocal of the LS fitted slope of the data plotted in this graph corresponds to coefficient T_{ri} (as explained in the text)

Slightly different fitting results are obtained by treating measured quantities as the dependent variable (instead of the independent variable), and since the correct procedure is to treat measured quantities as the dependent variable the presentation of Fig. 8, with the LS fit shown, is a correct treatment of the data under question. The LS fit of measured "r-i" as dependent variable to "R-I" as independent variable produces an intercept and slope having the following meaning.

$$r\text{-}i = C_3 + C_4 * (R\text{-}I) \tag{Eqn. 2}$$

Assume for the moment that we really want a way to calculate "R-I" from "r-i", as provided by Eqn. 1. Rearranging Eqn. 2 we are able to obtain the following relation:

$$R\text{-}I = (-C_3/C_4) + (1/C_4) * (r\text{-}i) \tag{Eqn. 3}$$

This has the form of a constant and slope, so let's rename terms to obtain the following.

$$R\text{-}I = C_{ri} + T_{ri} * (r\text{-}i) \tag{Eqn. 4}$$

where $C_{ri} = (-C_3/C_4)$ and $T_{ri} = (1/C_4)$. The term C_{ri} is called a "zero point offset" and as will be shown below it is unimportant (since it cancels out in subsequent derivations). The term T_{ri} is a transformation coefficient of first order importance. T_{ri} may be thought of as the rate of change of (R-I) with respect to (r-i), as is apparent from Fig. 7. For a "perfect system" $T_{ri} = 1$. The data in Fig. 8 produce a value for T_{ri} = 0.951 ± 0.046. This value is slightly smaller than 1 (but the difference from 1.00 is not statistically significant), consistent with Fig. 7, and that implies that for the reddest stars (i.e., those have large R-I), it is necessary to correct their apparent "r-i" by attributing to them a slightly smaller redness (*i.e.*, attributing to them an R-I that is smaller than r-i).

The reader is justified in wondering why so much effort went into deriving a value for something called T_{ri}. Be patient. We are really after an equation that permits us to convert r and i to R and I. What we've done so far is just part of our journey to understanding how this ultimate objective can be achieved.

Deriving Something Called T_r

Consider another plot showing something related to the error we appear to have in measured "r" as a function of known star color R-I.

EVALUATION OF Tr USING M67
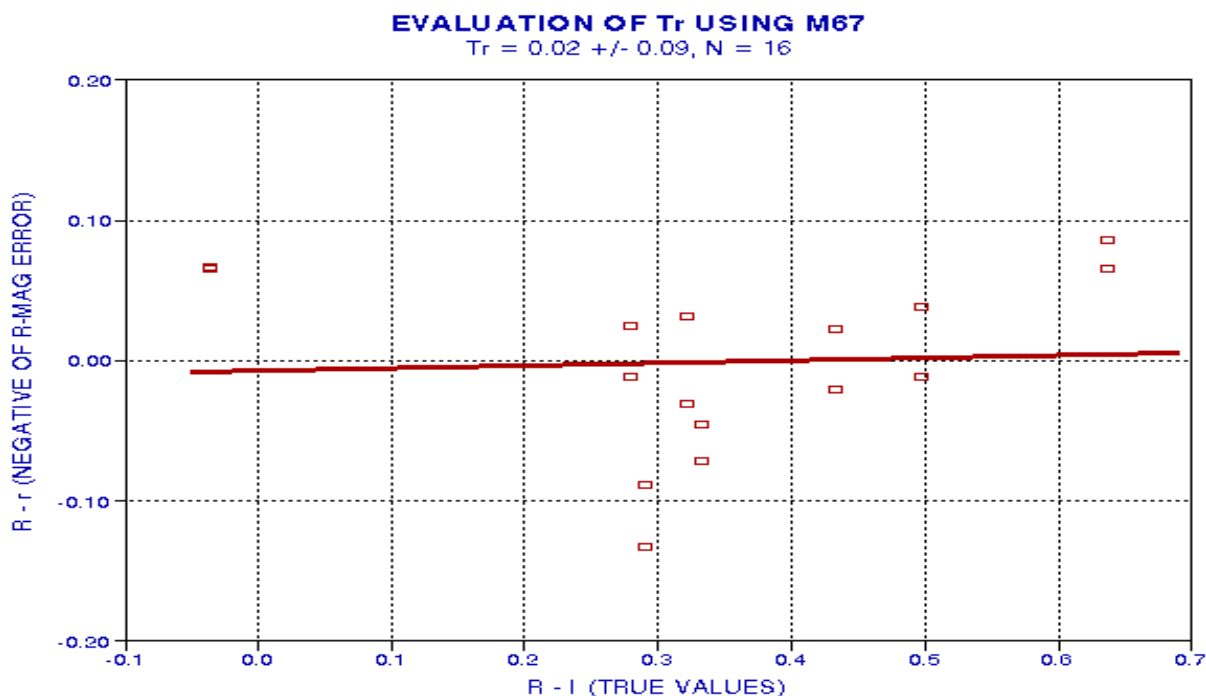Tr = 0.02 +/- 0.09, N = 16

Figure 9 - The same measurements are used to show that a correction is required to convert measured "r" to true "R" and that this correction depends on the star's R-I color. The LS fitted slope of the data graphed here corresponds to coefficient T_r.

We notice that in this plot the measured quantity is plotted on the Y-axis, so that if error bars were used they'd be vertical. Any LS fit to this data using "R-r" as the dependent variable and "R-I" as the independent variable will be compatible with a proper treatment of observation uncertainties. In other words, our LS slope fit will provide a correct relation between the two variables. The formal LS fit has a solution:

$$(R-r) = C_r + T_r * (R-I) \tag{Eqn. 5}$$

where the intercept and slope have been given the names C_r and T_r. The solution values for the data in Fig. 9 are C_r = -0.01 and T_r = +0.02 ± 0.09. The slope term is insignificantly different from zero (value/SE = 0.22).

We've just done something without stating why we did it. We produced a scatter diagram that contains different information than the first scatter diagram, with the hope that it might be useful. Now we're ready to combine equations 4 and 5 to arrive at a more useful result.

Deriving an Algorithm for Calibrating Magnitude Measurements of an Interesting Unknown Object, 2-Color Case

Consider two stars in the same CCD image, for which we shall use subscripts j and k. Assume we have calculated magnitudes (without worrying about a correct offset) that allow us to form color difference magnitudes (r-i) for each star: $(r-i)_j$ and $(r-i)_k$. Using Eqn. 4, we have:

$$(R-I)_j = T_{ri} * (r-i)_j + C_{ri} \tag{Eqn. 6}$$

$$(R-I)_k = T_{ri} * (r-i)_k + C_{ri} \tag{Eqn. 7}$$

Subtracting one from the other yields,

$$(R-I)_j - (R-I)_k = T_{ri} * [(r-i)_j - (r-i)_k] \tag{Eqn. 8}$$

Before making use of this difference magnitude equation, we must do something similar with Eqn. 5.

$$(R-r)_j - (R-r)_k = T_r * [(R-I)_j - (R-I)_k] + (C_r - C_r) \tag{Eqn. 9}$$

Suppose that star "k" is a comparison star with known magnitudes and star "j" is an object of interest, such as a supernova whose calibrated magnitude we want to determine. Let's rewrite Eqn. 9, replacing subscripts "j" and "k" with subscripts "s" and "c" (for "supernova" and "comparison star"), and also placing the subscripts with each magnitude.

$$(R_s - r_s) - (R_c - r_c) = T_r * [(R_s - I_s) - (R_c - I_c)] \tag{Eqn. 10}$$

and rearranging,

$$R_s = r_s + (R_c - r_c) + T_r * [(R_s - I_s) - (R_c - I_c)] \tag{Eqn. 11}$$

Notice in Eqn. 11 that the right side has only one "unknown" term: $(R_s - I_s)$. But "help is on the way" for notice Eqn. 8 can be written as

$$(R_s - I_s) - (R_c - I_c) = T_{ri} * [(r_s - i_s) - (r_c - i_c)] \tag{Eqn. 12}$$

and all terms on the right side are either known or measured. Substituting Eqn. 12 into Eqn. 11 yields

$$R_s = r_s + (R_c - r_c) + T_r * T_{ri} * [(r_s - i_s) - (r_c - i_c)] \tag{Eqn. 13}$$

and now all the terms on the right side are either known or measured. In other words, Eqn. 13 is a solution for the interesting object's R-magnitude, R_s. To solve for the interesting object's I-magnitude, I_s, notice the trivial relation

$$I_s = R_s - (R_s - I_s) \qquad\qquad\qquad\qquad\qquad\qquad \text{(Eqn. 14)}$$

All terms on the right side have been solved for above, so we also have a solution for the interesting object's I-magnitude, I_s, as well as its R-magnitude, R_s.

Here's where we stand: We've derived a procedure for determining an interesting (unknown) object's I and R magnitudes from the measurement of "i" and "r" magnitudes (without knowing offsets for either magnitude) for the interesting object and a comparison star having known (or at least "given") I and R magnitudes. In order to reduce stochastic uncertainties we can repeat this procedure using several comparison stars, then average the several results for I_s and R_s. This is an example of using transformation equations to achieve 2-color photometry of an interesting, unknown object.

The same concepts can be used for deriving calibrated magnitudes using <u>any</u> two neighboring filters.

Before deriving those other filter combination solutions, let's consider what was involved in the 2-color solution. It looks like a lot of work just to arrive at two numbers, I_s and R_s, but it's really not as daunting as it seems. Once the algorithm is implemented in a spreadsheet the user merely enters measured and given numbers into labeled cells, and the answer "pops out" without effort. The hard work is in deriving the algorithm, which only has to be done once. One purpose served by this "baby-step derivation" is to show that there is indeed sufficient information available to actually perform the calibration. With this knowledge there is an incentive to arrive at alternative algorithms to achieve an equivalent, or possibly better, solution. The last section of this document presents such an algorithm.

Algorithm for Calibrating V Measured Magnitudes

The procedure just described for calibrating measured "r" and "i" magnitudes of an interesting object (leading to R_s and I_s) can serve as a model for 2-color photometric calibration of an object's measured V-magnitude, "v". We merely substitute V and R for R and I in every instance of the previous solution (and similarly, substitute "v" and "r" for "r" and "i"). When this is done, we obtain the following (using actual measurements as illustration).
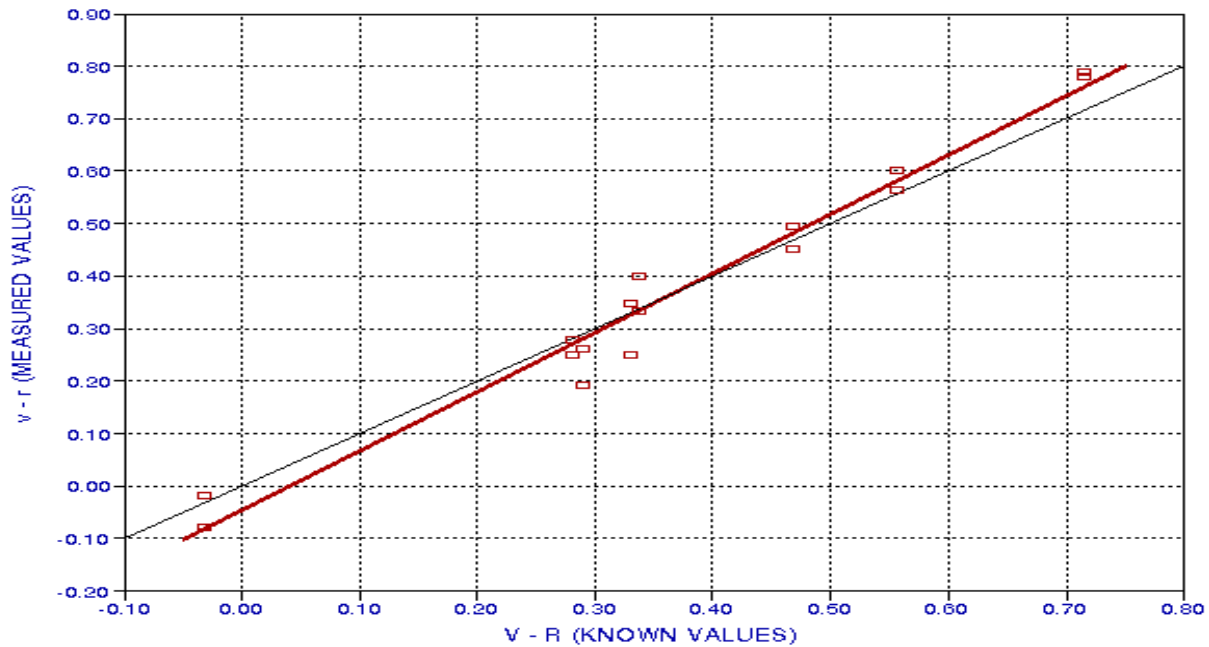
Figure 10 - Measured "v-r" versus known "V-R" for a group of comparison stars in M67. The reciprocal of the LS fit slope for this plot corresponds to coefficient T$_{vr}$

In this figure the reciprocal of the LS solution for slope corresponds to coefficient T$_{vr}$ = 0.888 ± 0.041. T$_{vr}$ may be thought of as the rate of change of (V-R) with respect to (v-r).
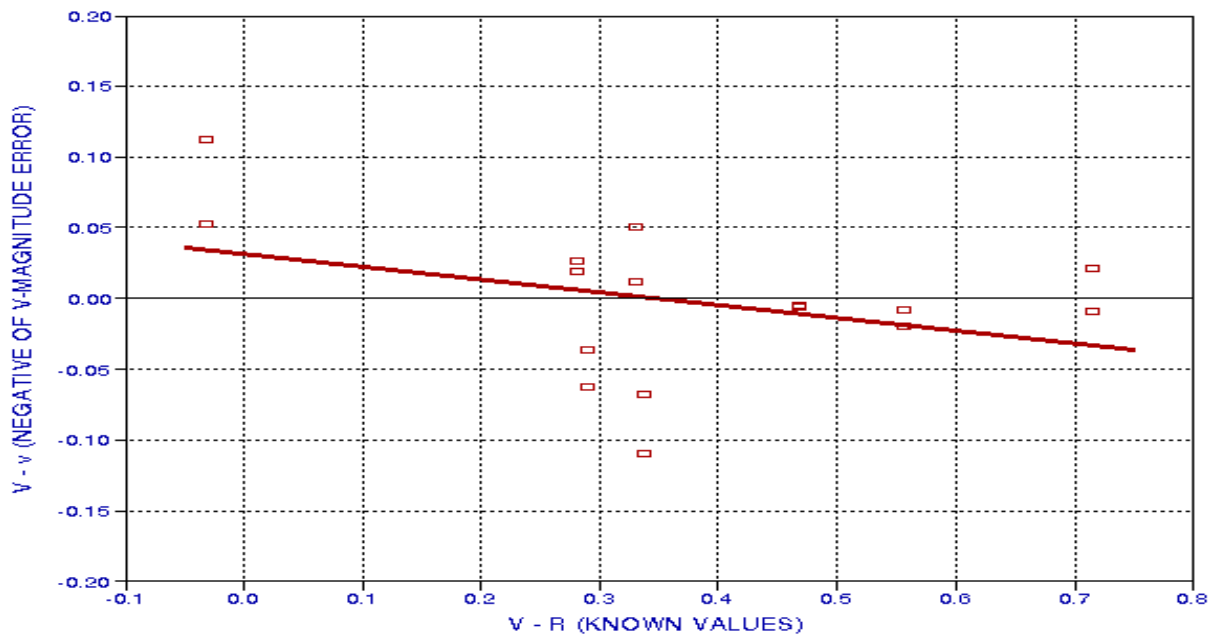

Figure 11 - Plot of "V-r" (known V magnitude minus measured "v") versus known "V-R" for a group of comparison stars in M67. The LS fitted slope corresponds to coefficient T$_v$.

The data in this figure has a LS fitted slope of -0.09 ± 0.06, which corresponds to the coefficient T_v. This solution for T_v is statistically compatible with zero, but it is better to use whatever the solved-for value.

Knowing T_{vr} and T_v allows for the following solution:

$$V_s = v_s + (V_c - v_c) + T_v * T_{vr} * [(v_s - r_s) - (v_c - r_c)] \qquad \text{(Eqn. 15)}$$

where all terms on the right side are either known or measured. This can be repeated for several comparisons stars, allowing for an average V_s solution. We've already solved for R_s, in the previous section, so it is not necessary to produce the counterpart to Eqns. 12 and 14. By foregoing a second solution for R_s based on a scatter plot of "R-r" versus "V-R" we are assuming that a star's I magnitude has more effect on its V-magnitude error than the star's V-magnitude. I'm unaware of a justification for this, but it is something to keep in mind.

Algorithm for Calibrating B Measured Magnitudes

Assuming an object's measured B-magnitude is most influenced by its V-magnitude, we need to determine only the coefficient T_{bv}, the rate of change of (B-V) with respect to (b-v). This can be visualized using the following graph.
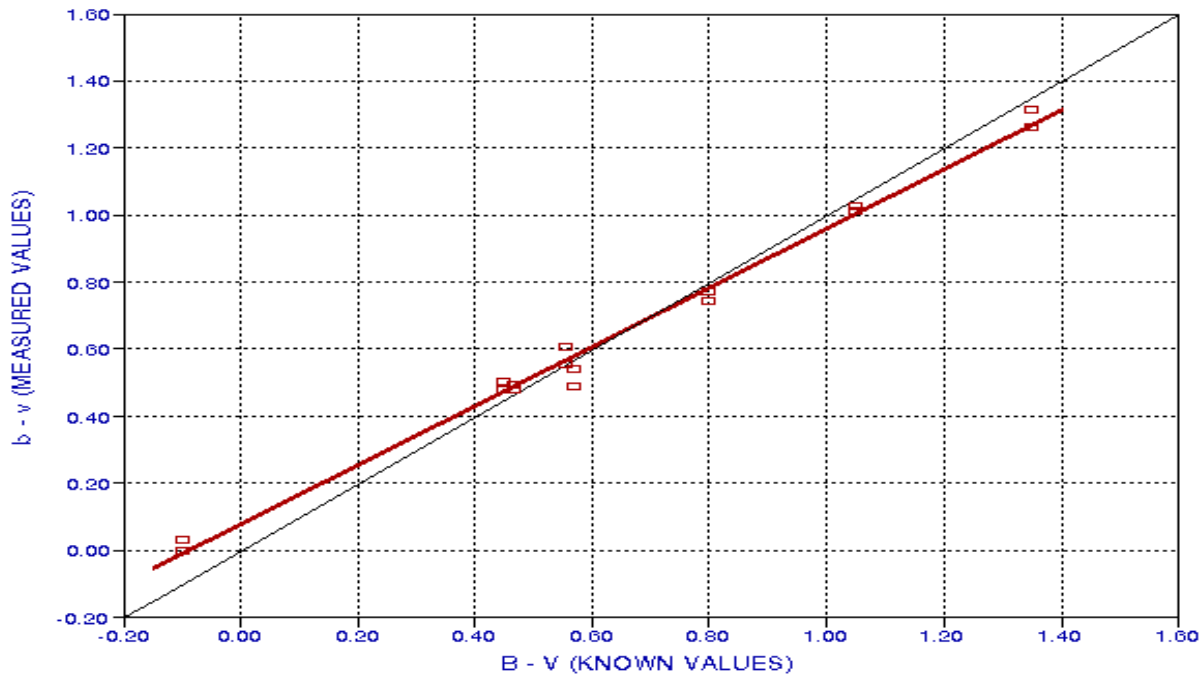

Figure 12 - Measured "b-v" versus known "B-V" for a group of comparison stars in M67. The reciprocal of the LS fit slope for this plot corresponds to coefficient T_{bv}

The reciprocal of the LS fitted slope of Fig. 12 corresponds to coefficient T_{bv}. Using the concepts embodied in Eqn. 12, we can solve for the term $(B_s - V_s)$ to obtain a solution for B_s.

$$B_s = V_s + (B_c - V_c) + T_{bv} * [(b_s - v_s) - (b_c - v_c)] \qquad \text{(Eqn. 16)}$$

The terms on the right side are either known or measured, so this equation affords a solution for B_s. Again, we are not taking into account a possible influence of the star's U-magnitude, and in this case there seems ample justification since few (if any) stars are brighter at wavelengths shorter than the B-magnitude filter pass band, whereas in most cases stars are brighter within the V-magnitude filter band pass than within the B-magnitude band pass. (The term "brightness" is used here to refer to the number of photons coming from the star at wavelengths within the band pass under consideration, weighted by the filter's response over that band pass; since photons in the visual region dislodge no more than one electron per photon, the energy per photon is not relevant.)

Summary of Coefficient Definitions

Here's a summary of how transformation equation coefficients are determined from comparisons star observations:

T_r = slope of (R-r) plotted versus (R-I)
T_v = slope of (V-v) plotted versus (V-R)
T_{ri} = reciprocal of slope of (r-i) plotted versus (R-I)
T_{vr} = reciprocal of slope of (v-r) plotted versus (V-R)
T_{bv} = reciprocal of slope of (b-v) plotted versus (B-V)

Summary of Implementing CCD Transformation Equations for the BVRI Case

Assume that an image contains several comparisons stars with known values for B, V, R and I. In the equations below each comparison star's known magnitudes are referred to below as B_c, V_c, R_c and I_c. Assume further that we have measured magnitudes b, v, r and i (with unknown offsets for each filter category) for each comparison star. These will be referred to below as b_c, v_c, r_c and i_c. Finally, we have measured magnitudes of our target object (sharing the same unknown offsets per filter category as apply to the comparisons stars). These will be referred to below as b_s, v_s, r_s, and i_s (where subscript "s" can be thought of as referring to fast-changing supernova). The task is to convert this data set to calibrated B_s, V_s, R_s and I_s for the object of interest. Here's the procedure derived above, and recommended by the AAVSO.

$(R_s - I_s) = (R_c - I_c) + T_{ri} * [(r_s - i_s) - (r_c - i_c)]$ (Eqns. 17a - 17e)
$R_s = r_s + (R_c - r_c) + T_r * [(R_s - I_s) - (R_c - I_c)]$, using the solution for $(R_s - I_s)$ in the above line
$I_s = R_s - (R_s - I_s)$, using R_s from the line above, and $(R_s - I_s)$ from the first line
$V_s = v_s + (V_c - v_c) + T_v * T_{vr} * [(v_s - r_s) - (v_c - r_c)]$
$B_s = V_s + (B_c - V_c) + T_{bv} * [(b_s - v_s) - (b_c - v_c)]$

IV. Equations for Other Filter Combinations

The foregoing assumed the observer made measurements in the all 4 colors, BVRI. Suppose an observer measures only VRI, BVR, or BV, or VR, or RI? What transformation equations should be used in those cases?

The logic of the previous section has the implicit assumption that a measurement is most affected by the objects brightness at longer wavelengths; which is to say, when correcting a magnitude measurement it is most useful to assume that the measurement using the filter at the next longer wavelength contains the information required for performing the correction. Thus, if the observations are VRI then V is most

influenced by R, and R is most influenced by I. The influence of V upon R is ignored. Given this "philosophy" we can re-map the VRI situation to that of VRI treated in the previous section. The following CCD transformation equations were constructed this way (you may encounter other formulations of the same equations producing the same result).

VRI Combination

For the VRI filter combination, the following version of CCD transformation equations can be used:

$$(R_s - I_s) = (R_c - I_c) + T_{ri} * [(r_s - i_s) - (r_c - i_c)]$$ (Eqns. 18a - 18d)
$$R_s = r_s + (R_c - r_c) + T_r * [(R_s - I_s) - (R_c - I_c)], \text{ using the solution for } (R_s - I_s) \text{ in the above line}$$
$$I_s = R_s - (R_s - I_s), \text{ using } R_s \text{ from the line above, and } (R_s - I_s) \text{ from the first line}$$
$$V_s = v_s + (V_c - v_c) + T_v * T_{vr} * [(v_s - r_s) - (v_c - r_c)]$$

where the definitions for T_{ri}, T_{vr}, Tr and T_v are the same as given above.

BVR Combination

For the BVR filter combination, the following version of CCD transformation equations can be used:

$$(V_s - R_s) = (V_c - R_c) + T_{vr} * [(v_s - r_s) - (v_c - r_c)]$$ (Eqns. 19a - 19d)
$$V_s = v_s + (V_c - v_c) + T_v * [(V_s - R_s) - (V_c - R_c)], \text{ using the solution for } (V_s - R_s) \text{ in the above line}$$
$$R_s = V_s - (V_s - R_s), \text{ using } V_s \text{ from the line above, and } (V_s - R_s) \text{ from the first line}$$
$$B_s = V_s + (B_c - V_c) + T_{bv} * [(b_s - v_s) - (b_c - v_c)]$$

where the definitions for T_{vr}, T_{bv} and T_v are the same as given above.

RI Combination

For this combination (treated above) we may use the following:

$$(R_s - I_s) = (R_c - I_c) + T_{ri} * [(r_s - i_s) - (r_c - i_c)]$$ (Eqns. 20a - 20c)
$$R_s = r_s + (R_c - r_c) + T_r * [(R_s - I_s) - (R_c - I_c)], \text{ using the solution for } (R_s - I_s) \text{ in the above line}$$
$$I_s = R_s - (R_s - I_s), \text{ using } R_s \text{ from the line above, and } (R_s - I_s) \text{ from the first line}$$

where the definitions for T_{ri} and T_r are the same as given above.

VR Combination

For this combination we may use the following:

$$(V_s - R_s) = (V_c - R_c) + T_{vr} * [(v_s - r_s) - (v_c - r_c)]$$ (Eqns. 21a - 21c)
$$V_s = v_s + (V_c - v_c) + T_v * [(V_s - R_s) - (V_c - R_c)], \text{ using the solution for } (V_s - R_s) \text{ in the above line}$$
$$R_s = V_s - (V_s - R_s), \text{ using } V_s \text{ from the line above, and } (V_s - R_s) \text{ from the first line}$$

In this case the definitions for T_{vr} and T_v are the same as given above.

BV Combination

For this combination we may use the following:

$(B_s - V_s) = (B_c - V_c) + T_{bv} * [(b_s - v_s) - (b_c - v_c)]$ (Eqns. 22a - 22c)
$B_s = b_s + (B_c - b_c) + T_b * [(B_s - V_s) - (B_c - V_c)]$, using the solution for $(B_s - V_s)$ in the above line
$V_s = B_s - (B_s - V_s)$, using B_s from the line above, and $(B_s - V_s)$ from the first line

Here the definition for T_{bv} is the same as given above, and T_b is the LS slope fit of (B-b) versus (B-V).

V. M67 Calibration Stars

The graphs in Section III illustrating the determination of transformation equation coefficients are based on actual measurements of the M67 color calibration stars. This section describes the 13 stars with well-established BVRI magnitudes that the AAVSO recommends for use as a primary standard. It is recommended that at least once per year this set of stars, or at least a sub-set of them, be observed and used to monitor changes in the observer's system calibration. Since M67 is most conveniently observed during the winter season, two other "secondary standard" star fields can be used at other times of the year.
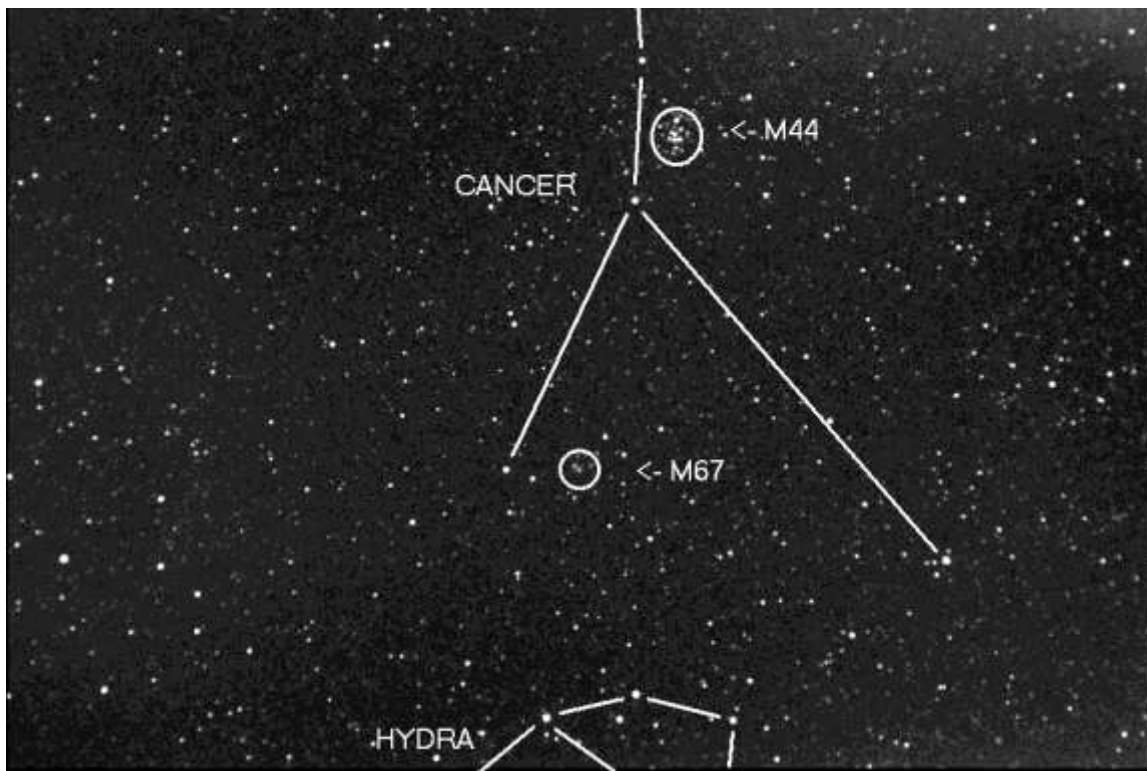
Figure 13 - Southern part of the constellation Cancer. M67 is a "smudge" at this resolution (160 arcseconds). The image is 21.3 degrees across.

Figure 14 - Zoom factor 1.5. Image size is 7.8 x 5.1 degrees. The faintest stars are magnitude 13.5. [SBIG ST-8E, Nikon 100 mm EFL, f/11, median combine of twelve 30-second exposures; 2002.05.08.3 UT, Santa Barbara residence]


Figure 15 - Zoom factor 3. Image size is 2.59 x 1.55 degrees. The faintest stars are 13th magnitude. Star FWHM = 18''arc. [SBIG ST-8E, Nikon 300 mm EFL, f/11, median combine of ten 30-second exposures; 2002.05.08.22 UT, Santa Barbara residence]

Figure 16. - Zoom factor 2.7 of the previous image. RGB color image size is 61.8 x 43.0 'arc. [Celestron CGE-1400, HyperStar, SBIG CFW-8 & ST-8XE CCD; 2003.12.10Z, Hereford, AZ.]

Figure 17 - Zoom factor of 1.8, but using an actual telescope, showing only the M67 region, measuring 25.3 x 15.5 'arc, centered at ~8:51 and +11° 49' (resolution ~6''arc). [Meade LX200 10-inch SCT, f/6.3; SBIG ST-8E CCD, TrueTech Color Filter Wheel, Schuler BVR filters; 2002.04.22; Santa Barbara residence]
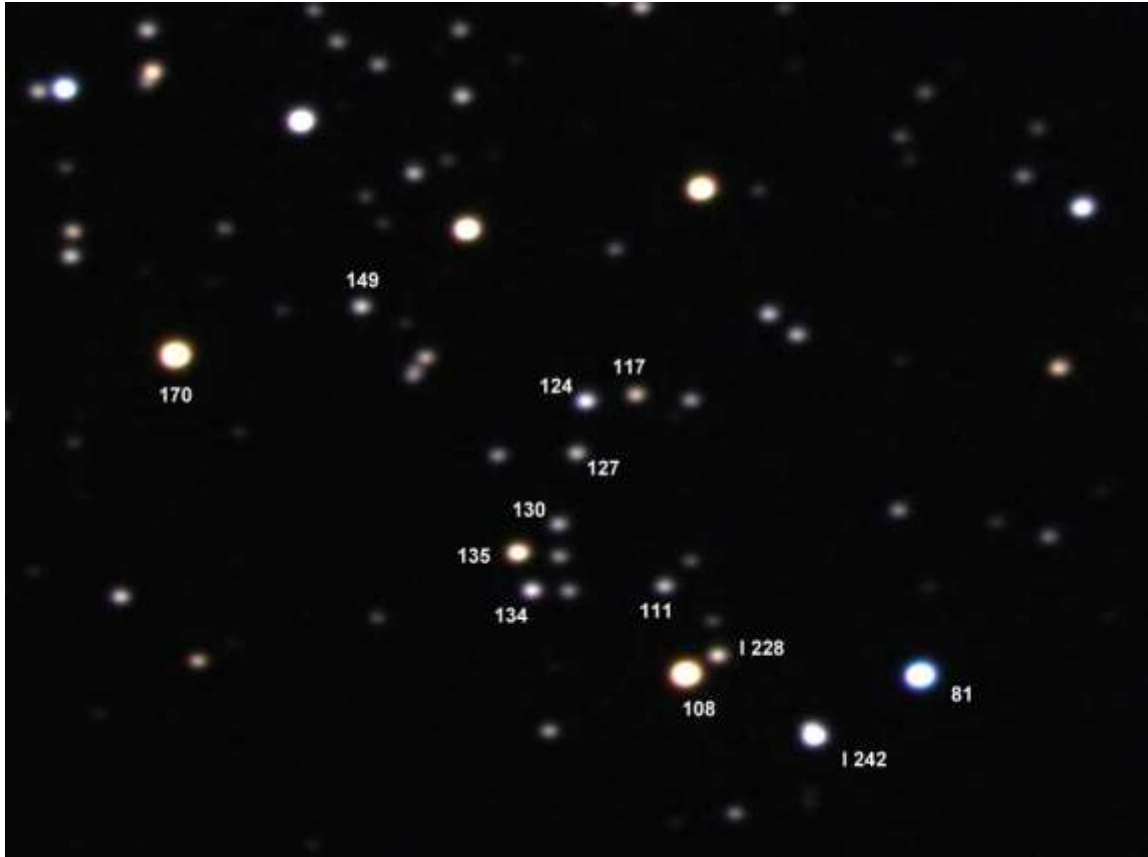
Figure 18 - Zoom of central region of previous image. Star #135 has coordinates 8:51:22, +11º 46' 06'' (epoch 2000.0). The image area is 6.82 x 4.85 'arc. The FWHM resolution is 4.0 ''arc in this sum of several 1-minute unguided exposures using BVR filters. The faintest stars have a visual magnitude of about 14. Stars to be used by AAVSO observers are indicated with star numbers. The bluest star is #81 and the reddest is #108. [LX200 10-inch SCT, f/6.3, SBIG ST-8E, True Tech filter wheel w/ Schuler BVRI filters; 2002.04.22Z, Santa Barbara, CA.]

The following table lists the M67 standard star magnitudes and colors for BVRI, in order of increasing V.

		B	V	R	I	B-V	V-R	R-I
1	170		9.663	8.961	8.336		0.702	0.625
2	108	11.052	9.701	8.986	8.350	1.351	0.715	0.636
3	81	9.929	10.027	10.059	10.095	-0.098	-0.032	-0.036
4	I242		10.884	10.616	10.351		0.268	0.265
5	135	12.487	11.436	10.880	10.383	1.051	0.556	0.497
6	124	12.584	12.118	11.838	11.558	0.466	0.280	0.280
7	134	12.825	12.256	11.919	11.587	0.569	0.337	0.332
8	I228		12.402	11.978	11.587		0.424	0.391
9	149		12.550	12.208	11.877		0.342	0.331
10	117	13.430	12.630	12.163	11.729	0.800	0.467	0.434
11	111		12.730	12.402	12.076		0.328	0.326
12	127	13.322	12.769	12.439	12.118	0.553	0.330	0.321
13	130	13.318	12.869	12.580	12.289	0.449	0.289	0.291

A subset of these stars was used for the analysis in Section III.

VI. Sample Data Analysis

In the previous section CCD transformation equation coefficients were derived from actual data made with a system consisting of a SBIG ST-8E CCD imager, Schuler photometry filters (Bu, V, Rs and Is), attached to Meade LX200 10-inch telescope (which I've also referred to as the "8E/Schuler" system). The coefficients that should be close to 1.00 (T_{ri}, T_{vr} and T_{bv}) were indeed close to the expected value, and the coefficients that were supposed to be close to zero (T_v and T_r) were indeed close to zero (this is shown in the table below). With such a system calibration corrections will be small.

In order to more easily demonstrate the need for calibrating using CCD transformation equations, I have chosen in this section to work with measurements made with the Meade 416XTE CCD and Meade color filter wheel (Model 616) blue and red filters with the Meade visual filter replaced by a good quality Optec visual filter (also referred to here as the "416XTE/616" system). This is the configuration that was NOT meant for photometry (as illustrated by Fig. 6), but which can in fact be used if care is taken with calibration.

The following table summarizes transformation equation coefficients for the "8E/Schuler" and "416XTE/616" systems.

COEFFICIENTS FOR TWO CCD/FILTER SYSTEMS

Coefficient	"8E/Schuler" System	"416XTE/616" System
T_{ri}	0.951 ± 0.046	n/a
T_{vr}	0.888 ± 0.041	0.987 ± 0.037
T_{bv}	1.136 ± 0.029	1.89 ± 0.13
T_r	$+0.019 \pm 0.088$	n/a
T_v	-0.090 ± 0.062	-0.015 ± 0.032

Notice that all Meade "416XTE/616" coefficients are close to the desired values except for T_{bv}. This is undoubtedly due to the filter/CCD's red-shifted spectral response (shown in Fig. 6). Incidentally, I believe in the old adage that "A measurement is not a measurement unless it comes with an uncertainty." All uncertainties quoted here are standard errors (stochastic component only).

The sample data used to illustrate the use of CCD transformation equations are for the supernova SN2002ap (0131+15), taken near the end of the period when a light curve could be made (due to the sun's slow march toward it). The measurements were made on the date 2002.03.09 UT. Dark and flat field corrections were of course made. MaxIm DL 3.0 was used to perform "aperture photometry" for 6 comparison stars as well as the SN, all of which were within the boundaries of each image. This is a BVR system, and the measured magnitudes for this date are:

"b" = 15.37
"v" = 14.30
"r" = 13.69

Although these magnitudes are not corrected using CCD transformation equations, they do reflect MaxIm DL's process of forcing them to have an offset that minimizes the RMS differences between all

comparisons star magnitudes and their known magnitudes (entered by the user). In other words, the MaxIm DL aperture photometry does a fit of all comparison star magnitudes to their known values and then produces an output of magnitudes for the comparison stars and the object of interest which do not require offset adjustments. It is my practice to record sets of magnitudes produced from several annulus choices. Each image may require carefully chosen annulus radii if the seeing was bad or if stars are near the comparison or object of interest. A spreadsheet is used to average the magnitudes from each annulus set (and inspect them for "outliers" - deserving rejection!). For the observations in question, the following figure shows how well the MaxIm DL magnitudes for the comparison stars agreed with their "known" magnitudes.
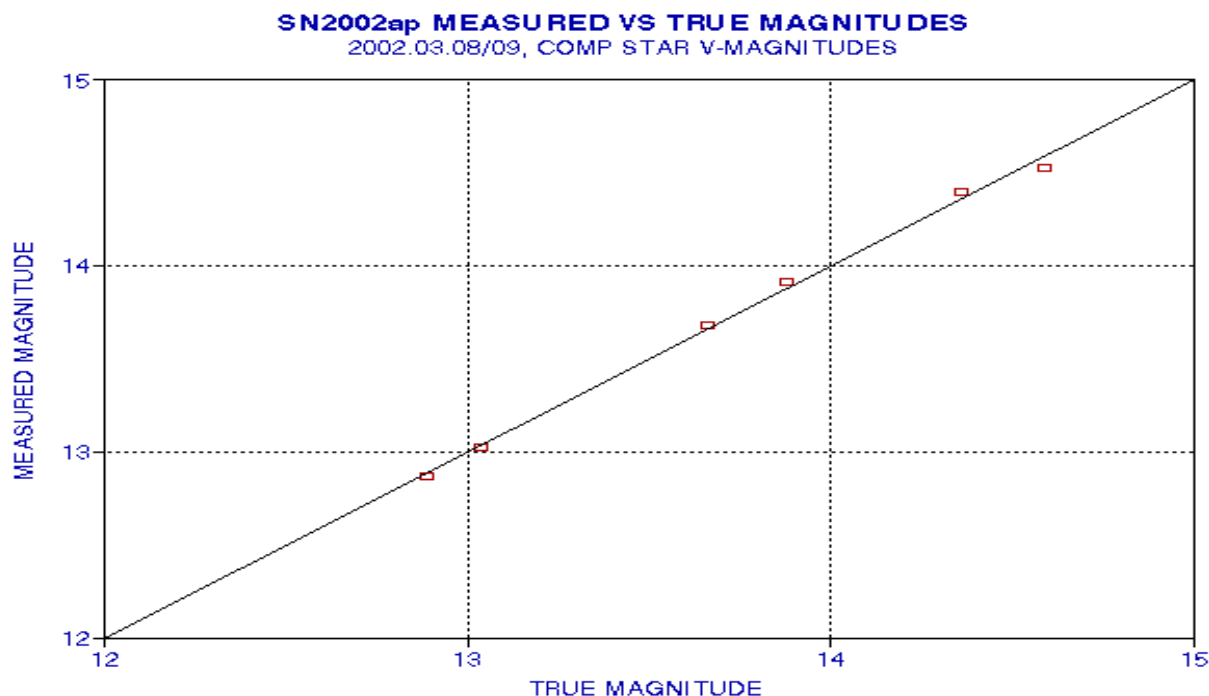

Figure 19 - Plot of "measured" versus "known" (or "true") visual magnitudes for comparison stars near object SN2002ap. RMS scatter off the 1:1 line is 0.039 magnitudes.

Some of the differences between measured and known magnitude for the comparisons stars is due to the colors of the comparisons stars, since at this stage the CCD transformation equations have not been used. Stochastic considerations predict an uncertainty of 0.019 magnitudes. The blue filter data exhibits greater departures from the 1:1 line that cannot be accounted for stochastically, implying that the color of the comparison stars have a greater effect upon measured blue magnitude (dealt with fully in the next section).

Since this is a BVR set of data, we shall use the following CCD transformation equations:

$(V_s - R_s) = (V_c - R_c) + T_{vr} * [(v_s - r_s) - (v_c - r_c)]$ (Eqns. 23a - 23d)
$V_s = v_s + (V_c - v_c) + T_v * [(V_s - R_s) - (V_c - R_c)]$, using the solution for $(V_s - R_s)$ in the above line
$R_s = V_s - (V_s - R_s)$, using V_s from the line above, and $(V_s - R_s)$ from the first line
$B_s = V_s + (B_c - V_c) + T_{bv} * [(b_s - v_s) - (b_c - v_c)]$

The comparison star known magnitudes, and the "measured" SN2002ap magnitudes, are given in the following table:

MEASURED AND KNOWN MAGNITUDES
For Observations of 2002.03.09 UT

Star	B-Magnitude	V-Magnitude	R-Magnitude
SN2002ap	15.37	14.30	13.69
130 Meas'd	13.86	13.03	12.60
146 Meas'd	15.12	14.53	14.19
137 Meas'd	14.35	13.68	13.29
139 Meas'd	14.73	13.91	13.41
129 Meas'd	13.66	12.87	12.51
144 Meas'd	15.15	14.40	13.96
130 Known	13.84	13.04	12.59
146 Known	15.18	14.59	14.25
137 Known	14.33	13.66	13.30
139 Known	14.82	13.88	13.38
129 Known	13.60	12.89	12.50
144 Known	15.09	14.36	13.95

Notice that the top half of the table consists of **measured** magnitudes (lower-case magnitudes), whereas the bottom half consist of "known" comparison star magnitudes (upper-case magnitudes). Star names are based on V-magnitude; i.e., star #130 refers to the star having V = 13.0 (actually, 13.04).

Let's first only consider the use of one comparison star, "130" in the table.

Eqn. 23a states that:

$$(V_s - R_s) = (V_c - R_c) + T_{vr} * [(v_s - r_s) - (v_c - r_c)]$$
$$(V_s - R_s) = (13.04 - 12.59) + 0.987 * [(14.30 - 13.69) - (13.03 - 12.60)]$$
$$= +0.6277$$

Eqn. 23b states that:

$V_s = v_s + (V_c - v_c) + T_v * [(V_s - R_s) - (V_c - R_c)]$, using the solution for $(V_s - R_s)$ in the above line
$V_s = 14.30 + (13.04 - 13.03) + (-0.015) * [(+0.628) - (13.04 - 12.59)]$
$= 14.3073$

Eqn. 23c states that:

$R_s = V_s - (V_s - R_s)$, using V_s from the line above, and $(V_s - R_s)$ from the first line
$R_s = 14.3073 - 0.6277$
$\quad = 13.6796$

Eqn. 23d states that:

$B_s = V_s + (B_c - V_c) + Tbv * [(b_s - v_s) - (b_c - v_c)]$
$B_s = 14.3073 + (13.84 - 13.04) + 1.89 * [(15.37 - 14.30) - (13.86 - 13.03)]$
$\quad = 15.5609$

The solution for Bs, Vs, and Rs, based on only the first comparison star, is therefore 15.561, 14.307 and 13.680.

Clearly, this is a job for a spreadsheet (or a program that reads data input files). My spreadsheet performed the above calculations for the other 5 comparison stars, producing results in the following table.

BVR SOLUTION FOR SN2002ap

Comp Star	B-Magnitude	V-Magnitude	R-Magnitude
130	15.561	14.307	13.680
146	15.853	14.356	13.750
137	15.703	14.277	13.700
139	15.681	14.268	13.660
129	15.555	14.316	13.680
144	15.592	14.257	13.680
Average =	**15.658**	**14.297**	**13.691**

The corrections in this case are ΔB, ΔV, $\Delta R = 0.29, 0.00, 0.00$ magnitudes. In other words, only the blue filter magnitude needed a correction, which must be attributable to the fact that the Meade "416XTE/616" system used a blue filter that was meant for pretty pictures instead of photometry. It is valid to ask the question "When a correction of 0.29 magnitudes is required, what's the uncertainty on the correction?" Intuitively, we should be prepared for an uncertainty as large as perhaps 0.10 magnitudes. When a filter spectral response is as far off as the one just used, it may be suggested that the "linear" relationships used by the CCD transformation equations may be inadequate to the task.

The next section picks up on this question, addresses it, and suggests an even simpler method than the traditionally-used CCD transformation equations.

VII. An Alternative to Transformation Equations That Include an Implicit Correction for Atmospheric Extinction

It must be common for hardware to dictate analysis procedure. When there's an advance in hardware, or software, there's a time lag before analysis procedures adapt and make use of new opportunities. The transformation equations must have been developed before CCDs, and before modern software programs such as MaxIm DL. When you're using a photoelectric tube to detect and amplify counts from photons, you're dealing with one star at a time. There would be a time penalty for any analysis procedure that relied upon many nearby comparison stars - even if they existed. Data analysis of each star, one at a time also represents a penalty for any analysis method that requires the use of many comparison stars.

Today, with large area CCD imagers and powerful analysis programs within the price range of amateurs, new analysis opportunities exist. I want to describe one that has a couple attractive features.

The CCD transformation equations have two shortcomings that should be kept in mind. First, they rely upon linear relationships, with no second order terms. Second, the transformation equations described above, suggested for use by amateurs, do not allow for changes in atmospheric extinction between the time coefficients are determined and the time that observations of a region of interest are made.

The principle underlying the transformation equation philosophy is that when the spectral response associated with an observation is uncertain, errors will appear that are caused by the fact that different stars have different spectral distributions. Some comparison stars will be blue, others will be yellow, and some will be red. Also, the object of interest will be of unknown color, until observations are made and reduced.

With MaxIm DL, aperture photometry can be performed on as many as 9 comparison stars at a time, plus up to 9 objects with unspecified magnitudes. Right away, it can be seen that "check stars" can be easily included in an analysis, merely by clicking on their image and specifying them to be "object" instead of "reference star." Many image files can be analyzed just as easily as one averaged image file. Imagine the opportunities afforded by having up to 9 comparison stars from the same CCD image. Well, better yet, let me illustrate one of them.

SN2002ap MEASURED VS TRUE MAGNITUDES
DATA OF 2002.02.20/21, REF STAR B-MAG'S
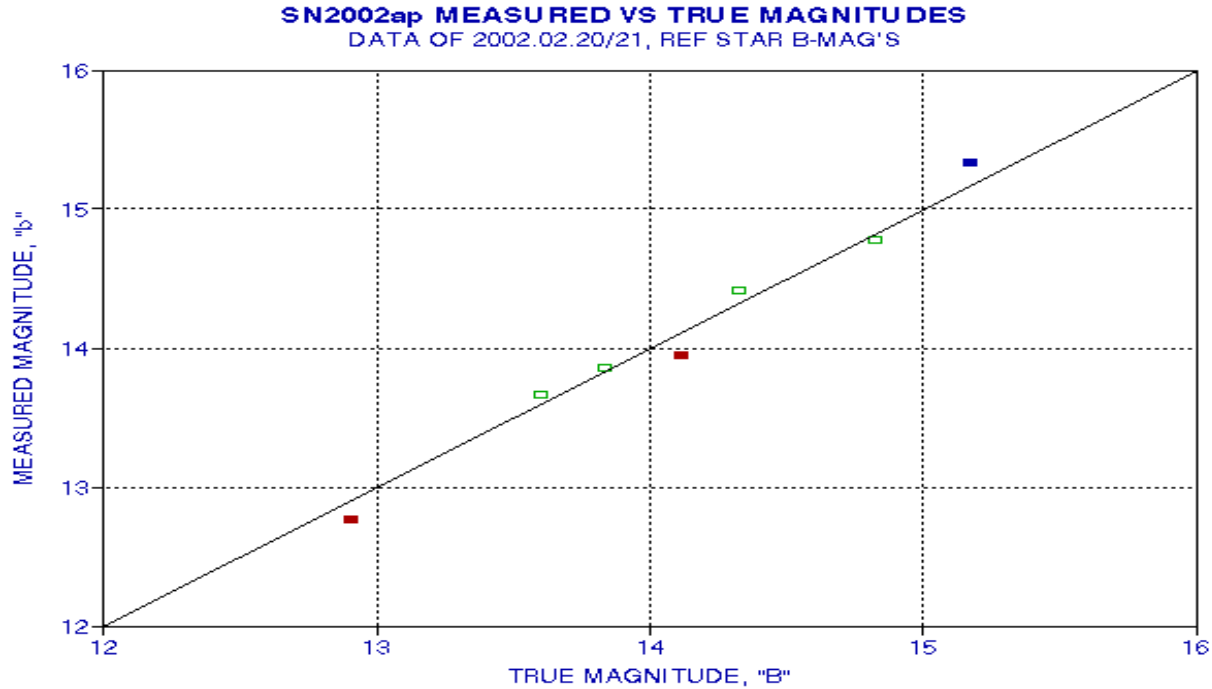
Figure 20 - Plot of measured magnitudes, "b", versus known magnitudes, "B" for 7 comparison stars in the same image as SN2002ap, using the Meade "416XTE/616" system. One comparison star has an especially small B-V (and is therefore "bluer" than the others), and it is plotted with a sold blue symbol. Two stars have especially large B-V (are redder than the others), and they are plotted using solid red symbols.

Anybody seeing Fig. 20 should notice that there's a pattern of "b" versus "B" wherein bluish stars are measured to be dimmer than they actually are and reddish stars are measured to be brighter than they actually are. This is what was predicted in the discussion section for the Meade "416XTE/616" system below Fig. 6. Could it be that the predicted behavior of a red-shifted Meade B-filter spectral response is apparent in this simple plot of magnitudes that came straight out of the MaxIm DL aperture photometry analysis? Take note that no complicated transformation equations have been employed in creating Fig. 20. One must wonder if there's a coherent pattern of "(b-B) versus (B-V)" using these comparison stars. Indeed, there are, as the next figure illustrates!

ERROR OF "b" FOR REFERENCE STARS
(b-B) = +0.64 - (B-V) +0.29 * (B-V) ^ 2
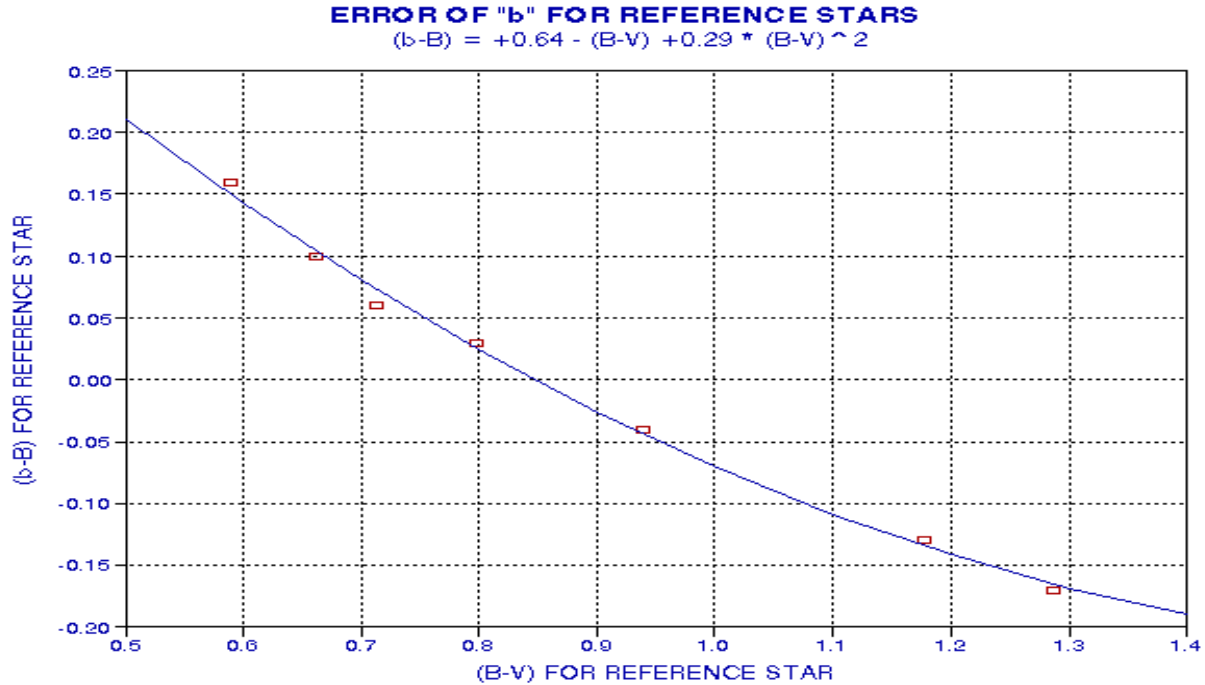
Figure 21 - Plot of "b-B" versus "B-V" for 7 comparison stars in the same image as SN2002ap. The equation for the second-order fitted curve is given below the figure title. The RMS difference of the data with respect to the fitted curve is 0.007 magnitudes. (Data was made using the Meade "416XTE/616" system.)

Clearly, the "b-B" differences are correlated with "B-V". In other words, "b" errors are correlated in a non-linear manner with comparison star B-V color. The empirical fit was determined easily using a spreadsheet's multiple regression features. This simple plot is conveying information about biases in the blue magnitude measurements. It is natural to wonder if it can be used, as it is, for correcting the SN2002ap measured blue magnitude. Since we don't yet know "B-V" for SN2002ap we can't just make a reading at a designated X-axis value. We at least need an estimate for "b-v". The V-filter images were also analyzed by MaxIm DL, and the following figure shows the scatter plot of measured "v" versus true "V" magnitudes.
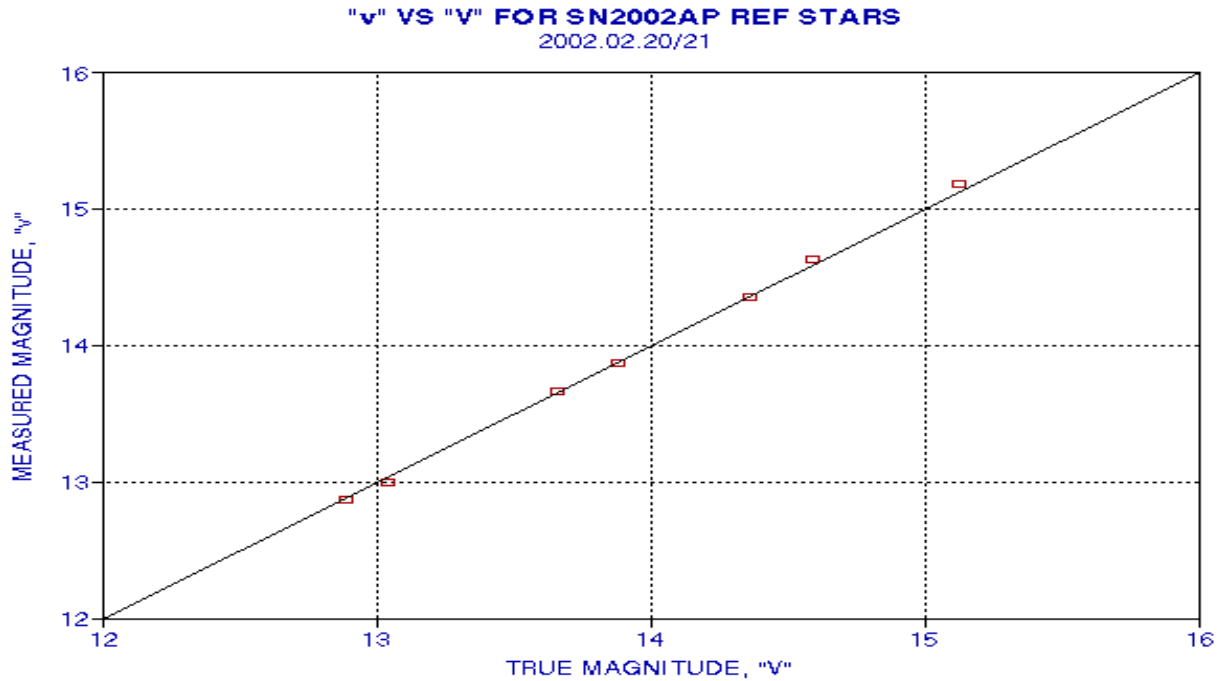
Figure 22 - Visible filter measured magnitude "v" versus known magnitude "V" for 7 comparison stars in the SN2002ap image. The RMS difference of the data with respect to the 1:1 line is 0.003 magnitudes. (Data was made using the Meade "416XTE/616" system.)

Fig. 22 shows that the measured V-magnitudes exhibit better behavior than the measured B-magnitudes (Fig. 20). In fact, it would appear that color effects are small, being less than the 0.036 magnitude RMS scatter of the data with respect to the 1:1 line. SN2002ap has a measured V-filter magnitude "v" of 13.094 ± 0.010 (stochastic SE). Since "b" is 14.266 ± 0.005 (stochastic SE), we now have "b-v" = 1.172 ± 0.012. This is a start in determining how to correct "b" for the blue bias shown in Fig. 21.

This may seem inelegant, but the following procedure works and it's quick and easy. We shall iterate ourselves to a solution! Let's make the assumption that "V" = "v", which was shown in the previous section to be a good one for this CCD/filter system. It will usually be the case that "v" is more accurate than "b" due to the fact that stellar spectra typically have steep slopes throughout the blue filter region, but are usually close to their peak flux near the visible filter region. If we assume that "V" = "v", then let's ask the question "What value of "B" will produce the measured "b" value, given the "b" bias curve of Fig. 20. Either an explicit iteration procedure can be created (within a spreadsheet or in the program that does the reduction) or a trial-and-error manual approach can be implemented. Only a few iterations lead to a result: B = 14.447, corresponding to B-V = 1.353, leading to a "b" error of -0.181, causing b = 14.266. This solution for B is therefore compatible with both the measured value "b" but also the error curve for b (the negative of what's plotted in Fig. 21).

ERROR OF "b" FOR REFERENCE STARS
(b-B) = +0.64 - (B-V) +0.29 * (B-V)^2
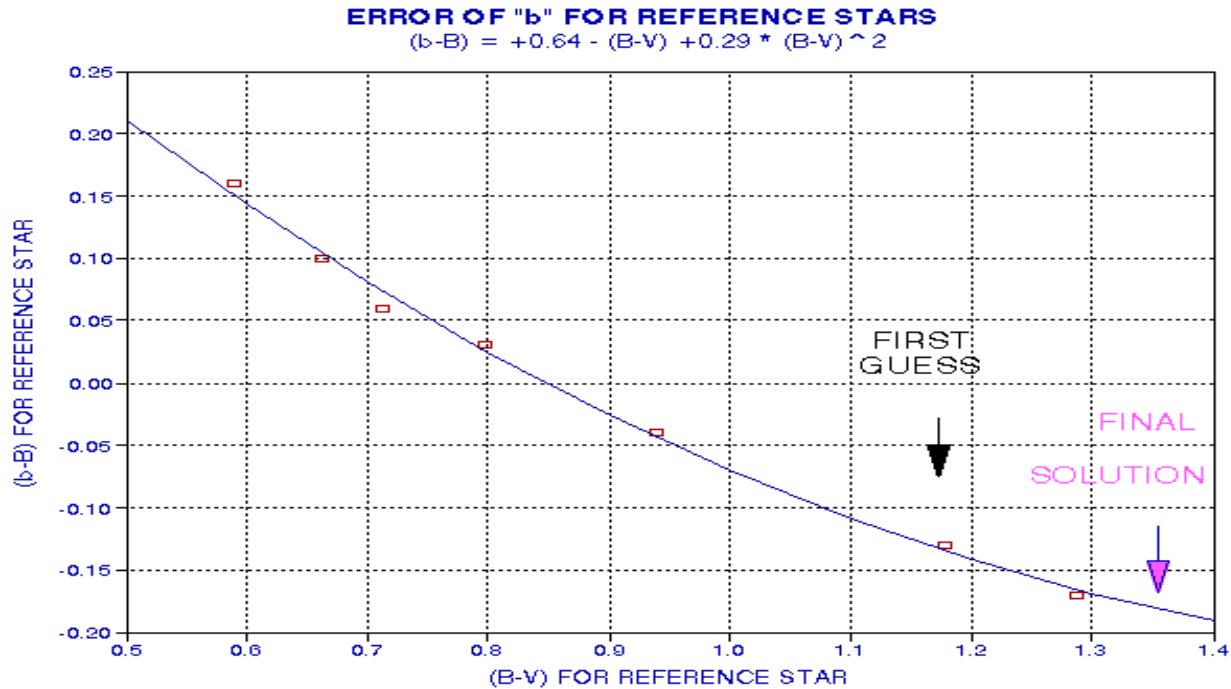
Figure 23 - Starting guess and ending estimate for SN2002ap's "B-V", leading to an estimate that for SN2002ap B-V = 1.353 (and since V = 13.094, B must be 14.447). (Data was made using the Meade "416XTE/616" system.)

Therefore, provided SN2002ap's v =V, we have arrived at an estimate that for SN2002ap B-V = 1.353, B =14.447 and the required correction to b is +0.181. Note that transformation equations were NOT used to determine this. As will be discussed below, the transformation equation solution for this date calls for a b-magnitude correction of +0.40 magnitudes, which differs from +0.181. However, there may be an explanation for this discrepancy, and the transformation equations are a good candidate for being in error - as described below.

Time-Out to Interject Some Comments

The procedure just described has weaknesses as well as strengths. First, I discuss the strengths.

Since the curve for (b-B) versus (B-V) was created using comparison stars close to the object in question, atmospheric extinction effects have been incorporated in the solution procedure. Presumably, if the observations were made under different conditions (a higher elevation angle, or wetter day, etc), the "(b-B) versus (B-V)" curve would be different. This is an attractive feature, since we want atmospheric extinction effects unique to the observations under analysis to be incorporated, even if they are incorporated implicitly instead of explicitly. Using the CCD Transformation Equations recommended by AAVSO, where there is no provision for extinction corrections, if the M67 calibration observations are done once per year, when M67 is high in the sky, the coefficients determined from these observations will be valid (subject to the limitations of using linear terms only) for only the same approximate conditions - namely, high elevation angle during winter (i.e., dry) atmospheric conditions. When the coefficients are used for low elevation observations, or during the summer (humid) season, the blue filter pass band will be shifted slightly to the red with respect to the time the M67 observations were made and coefficients were determined. This consideration argues in favor of attempting to use a more sophisticated procedure

- one that explicitly (or implicitly) takes into account atmospheric extinction effects (as "the professionals" do).

Second, the calibration procedure does not assume that the CCD/filter system has not changed since the last M67 calibration (used in establishing CCD transformation equation coefficients). In other words, using the new procedure described here it is not necessary to perform M67 calibrations at yearly or more frequent intervals. One caveat is that the assumption that v = V must be checked, and M67 calibration is a good way to do this.

Third, the reduction procedure was simple and can be performed quickly with less chance of typing errors.

Putting the Proposed New Calibration Method to the Test

If the proposed simpler method for calibrating photometry measurements has merit, it should at least pass some obvious self-consistency tests.

First, if a large dependence was found for (b-B) versus (B-V) for a sub-optimal system (employing a Meade B-filter not intended for photometry), then a smaller dependence should be found for (b-B) versus (B-V) using a better system (for example, the one employing Schuler filters that are intended for photometry). This prediction will be tested using the same M67 reference stars that were used in producing Fig. 20 and 21.

The following figure is the counterpart to Fig. 14, plotting "b" versus "B" for the set of M67 comparison stars.
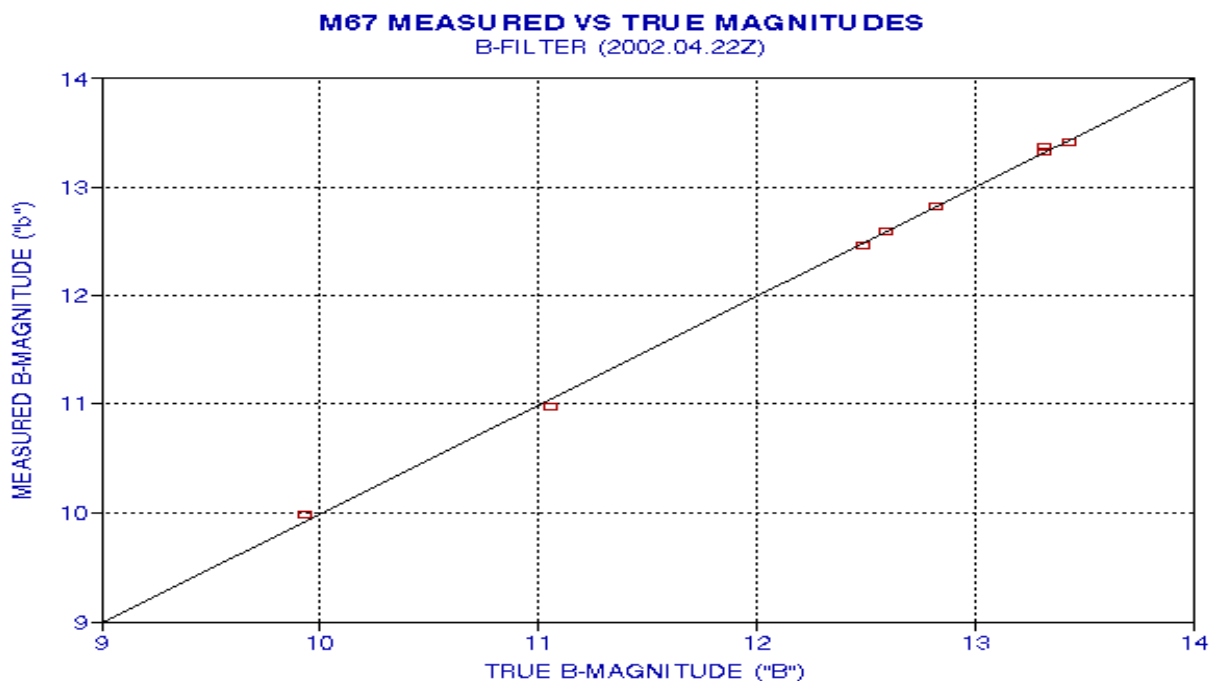
Figure 24 - Plot of measured "b" magnitudes versus M67 comparison star "B" magnitudes using the "8E/Schuler" system.

The scatter of this plot is to be compared with the scatter in Fig. 20. Clearly, the "8E/Schuler" system produces a better fit to the 1:1 line, implying that "good filters matter" and that the suggested alternative calibration procedure yields good quality "b" magnitudes using good filter data. The goal, of course, is to also be able to convert "b" magnitudes to "B" magnitudes when departures from the 1:1 line exist. The next figure shows that even when the "b" versus "B" scatter is small, a pattern of "b=B" versus "B-V" can be discerned, allowing for an even better determination of "B" from "b".
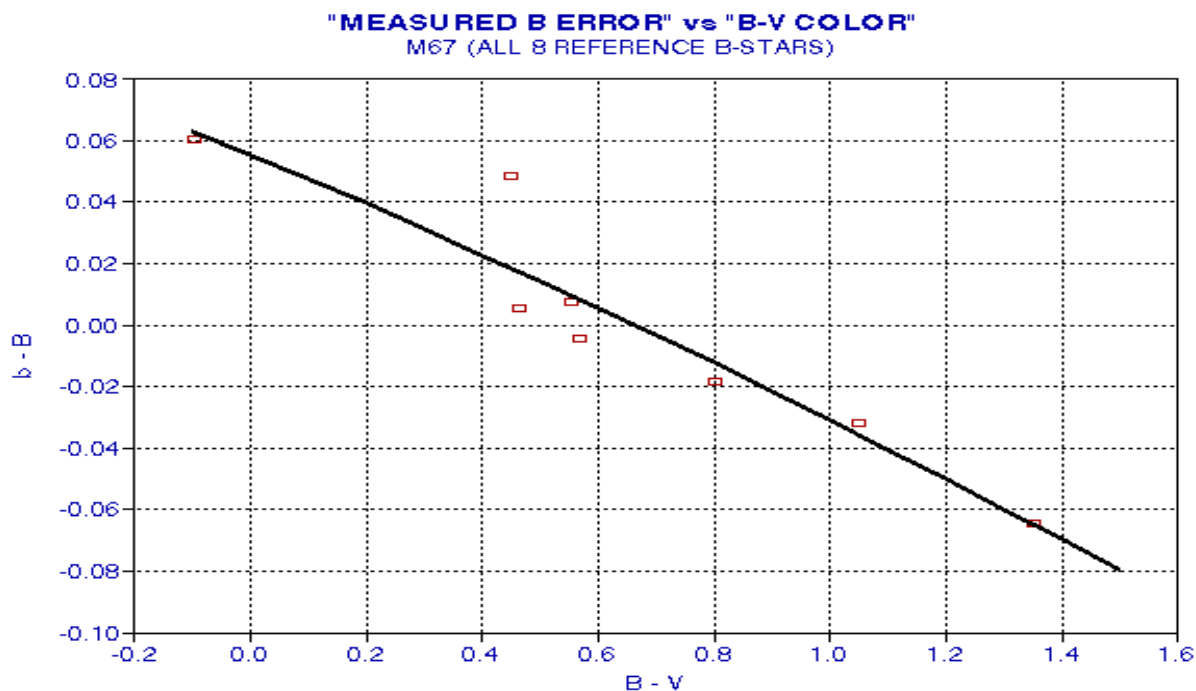
Figure 25 - Plot of (b-B) versus (B-V), i.e., dependence of measured "b" on B-V star color, for the "8E/Schuler" system
All 8 M67 reference stars with AAVSO recommended B-magnitudes are used to *determine a second-order fit.

The scatter of this plot is to be compared with the scatter in Fig. 21. It has two messages. First, using the suggested alternative calibration procedure it appears that "b" can be converted to "B" with a residual uncertainty of ~0.02 magnitudes. This is close to the stochastic uncertainty for the observations used, so a better inherent accuracy might be achievable using the suggested calibration method. Second, whereas the average (linear) slope of b-error versus (B-V) color in Fig. 21 is 0.50 magnitudes per magnitude, in Fig. 25 the average slope is 0.08 magnitudes per magnitude - i.e., 6 times smaller! (Figures 21 and 25 have different X-axis and Y-axis scale factors, so the visual appearance of the two may be deceiving.) The prediction is borne out by the data.

For another self-consistency check, if the proposed calibration method is to be depended upon it should always produce well-correlated linear relationships between large sets of well-behaved V-magnitudes. For example, in Fig. 22 only 7 M67 comparison stars were used to show that the MaxIm DL aperture photometry produces well-behaved V-magnitudes. The following figure shows that all 13 M67 comparison stars are well-behaved using the MaxIm DL aperture photometry.
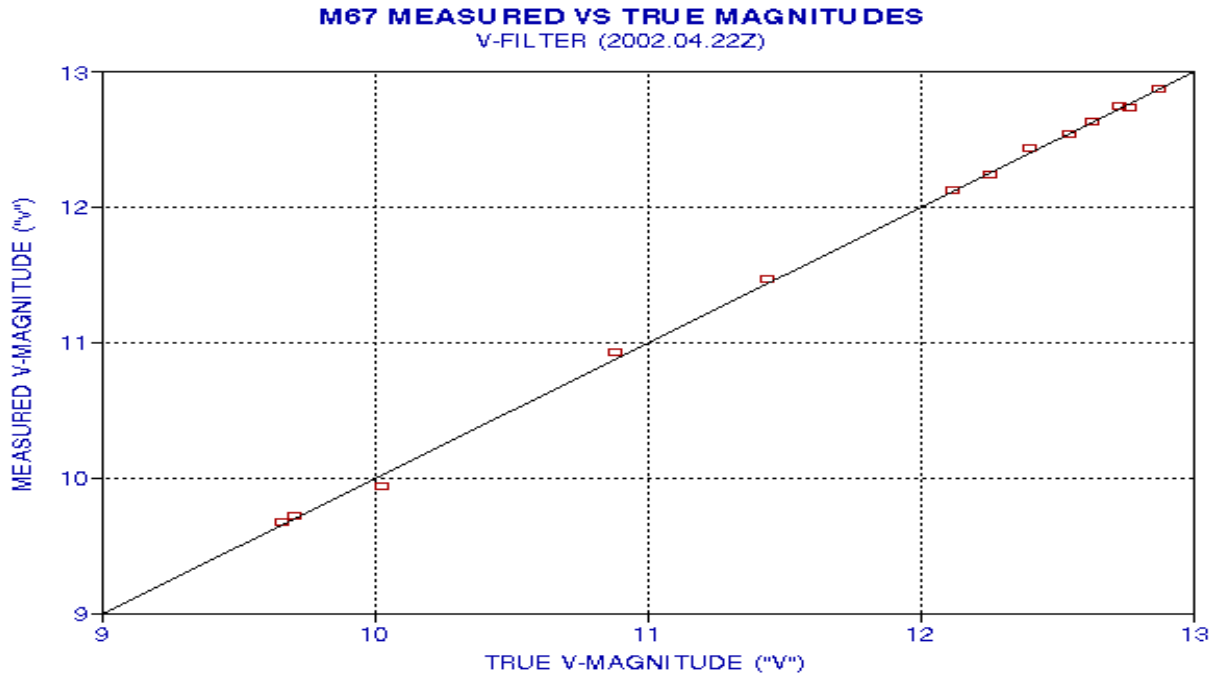
Figure 26 - All 13 M67 comparison stars were subjected to the MaxIm DL aperture photometry using a set of 3 V-filter images (using the "8E/Schuler" system) and the system solution for V-magnitudes is plotted versus "true" V magnitudes. The RMS difference with respect to the 1:1 line is 0.033 magnitudes.

The 13 M67 comparison stars exhibit an excellent correlation with the expected 1:1 line. The range of magnitudes is 3.3 (intensity ratio of 21), yet the RMS scatter off the 1:1 line is only 3%. Perhaps most of this scatter is due to a real dependence of v-error on B-R color, as the following figure suggests.
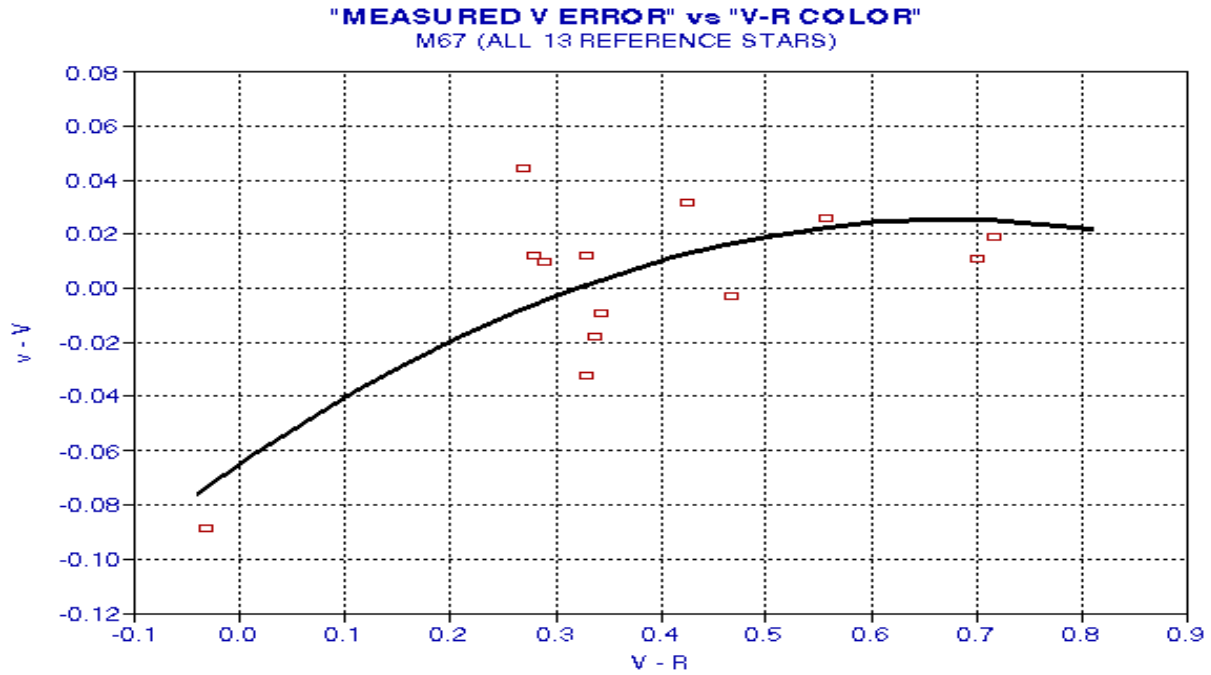
Figure 27 - Dependence of measured "v" magnitude error on V-R color for the "8E/Schuler" system and based on all 13 M67 comparisons stars.

A similar analysis can be performed with the red and infrared magnitudes, but first let's consider a concern that you might have about this entire procedure.

A potential objection to the proposed calibration method is that it must take lots of work to produce photometry of enough stars to produce a good second-order curve of magnitude error versus color. Consider the following "screen capture" figure.
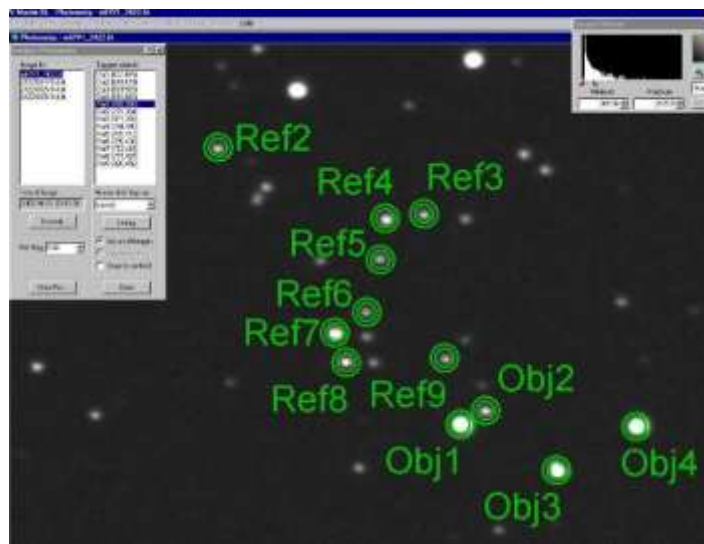

Figure 28 - Screen capture after specifying that MaxIm DL perform aperture photometry on 9 "reference" stars and 4 "Object" stars, corresponding to the 13 "comparison" stars in M67

After images are prepared (dark and flat field corrected, and averaging of those with the best "atmospheric seeing"), the procedure for performing photometry analysis (using MaxIm DL) is quite straightforward and involves little more work to do photometry on 13 stars, for example, than on one. The user "clicks" the stars to be used and then enters magnitudes for those assigned to "reference" status. Each click causes that star to be located and the annulus pattern for the star snaps to the centroid for all images to be used. After entering the reference star magnitudes (values from the comparison star list), the "View Plot" window button is clicked, and a window appears showing solved-for magnitudes for all stars. The S-by-I matrix of magnitude solutions (S number of stars by I number of images) can be saved to a text file in a specified directory. Later, these files can be imported to a spreadsheet (or read by a reduction program), and graphs can be produced like those in the previous figures. This entire process is quick and is not prone to errors. The most important decision the user must make is to specify the three annuli so that the outer background ring doesn't include nearby stars, etc. The large numbers of comparison stars that can be used with modern analysis programs like MaxIm DL make the proposed alternative calibration procedure much more feasible than it would have been just a few years ago.

Now, let's return to a demonstration of calibrating measured R and I magnitudes.
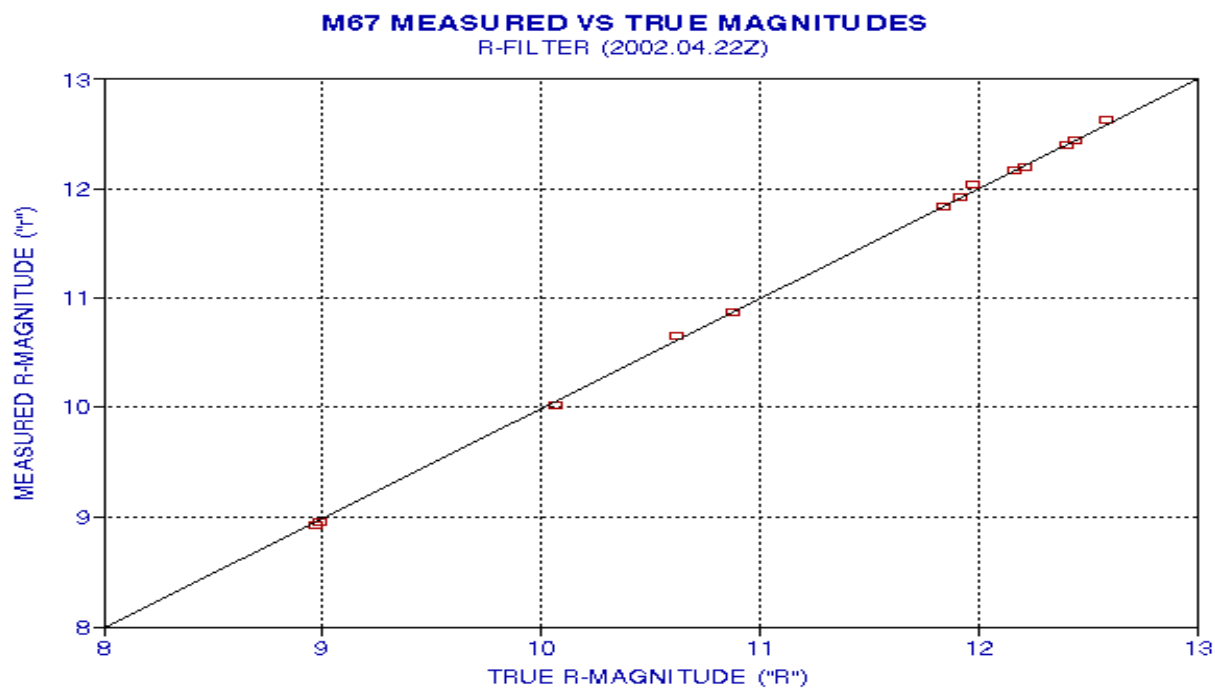
Figure 29 - All 13 M67 comparison stars were subjected to the MaxIm DL aperture photometry using a set of 7 R-filter images (using the "8E/Schuler" system) and the system solution for R-magnitudes is plotted versus "true" R magnitudes. The RMS difference with respect to the 1:1 line is 0.029 magnitudes.

From this plot it would appear that all measured "r" can be reliably converted to a standard R-magnitude without applying corrections (using the Schuler filters and SBIG ST-8E CCD). The expected residual error, based on the departures from the 1:1 line of this plot, is 0.029 magnitudes. The actual SE for a larger set of images could be less, considering that 0.029 magnitudes is the orthogonal sum of stochastic and bias errors, and the stochastic component will decrease with additional observations. Out of curiosity, however, let's view the difference magnitude versus known R-I color.

"MEASURED R ERROR" vs "R-I COLOR"
M67 (ALL 13 REFERENCE R-STARS)
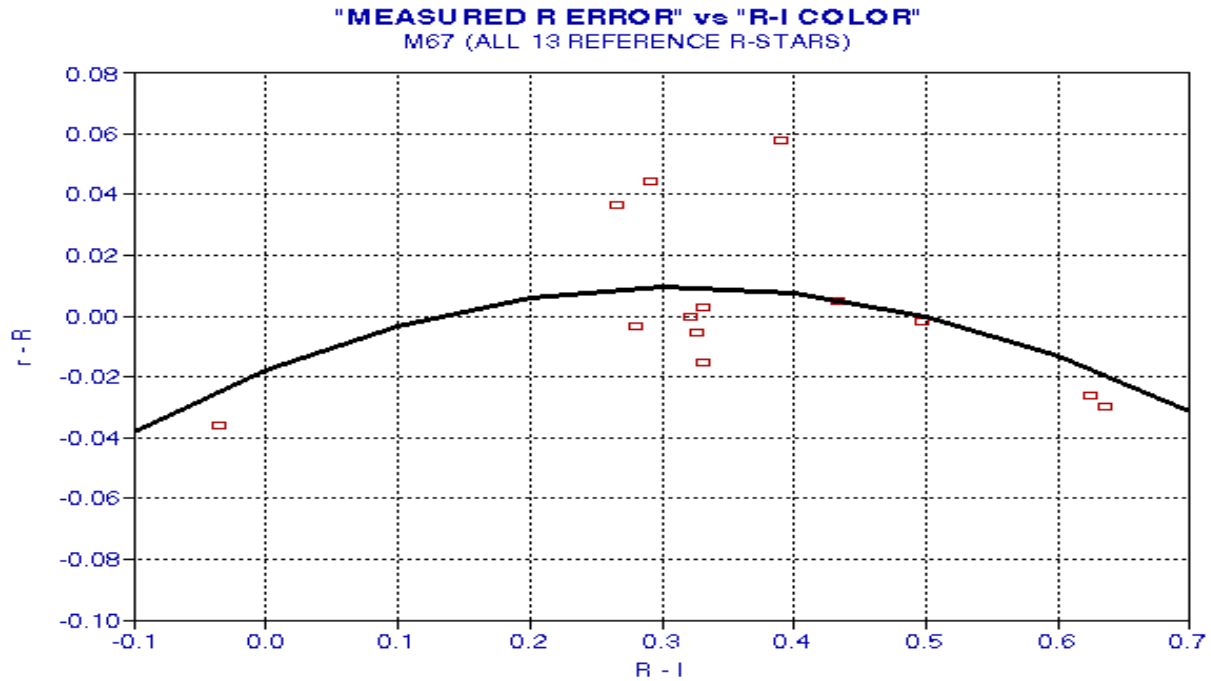
Figure 30 - Dependence of measured "r" magnitude error on R-I color for the "8E/Schuler" system and based on all 13 M67 comparisons stars (in 7 images).

These data exhibit a weak pattern for the "r - R" magnitude differences versus "R - I" color. The same negative curvature was found for "v-V" versus "V-R" (Fig. 27) and "b-B" versus "B-V" (Fig. 25). The fact that all three magnitude error versus color have the same curvature versus color suggests that the curvatures for each data set are real. The fact that the Meade B-filter exhibits the opposite curvature may simply reflect the dominating effect of a large red-shifted passband. If the fitted line in Fig. 30 is accepted, then we may surmise that it is possible to correct measured "r" with an accuracy of 0.02 magnitudes (the apparent RMS of the measurements with respect to the fitted line).

The following figure shows measured infrared magnitudes versus true infrared magnitudes.

M67 MEASURED VS TRUE MAGNITUDES
**I-FILTER (2002.04.22Z)**
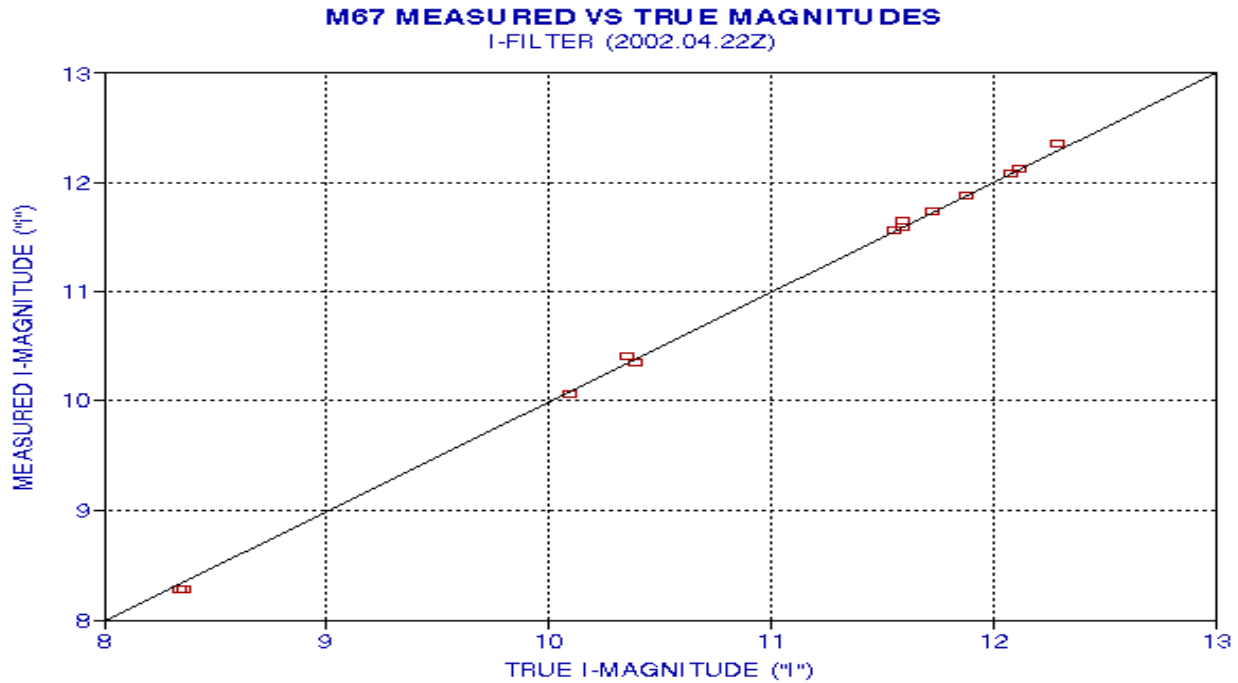
Figure 31 - All 13 M67 comparison stars were subjected to the MaxIm DL aperture photometry using a set of 8 I-filter images (using the "8E/Schuler" system) and the system solution for I-magnitudes is plotted versus "true" I magnitudes. The RMS difference with respect to the 1:1 line is 0.042 magnitudes.

The scatter of the infrared measurements with respect to "true" values is 0.042 magnitudes, which is slightly greater than the 0.029 magnitude SE for the red filter measurements. Do the "i-I" differences correlate with color? We don't have longer wavelength measurements for establishing color, but this is not a problem. After all, it was somewhat arbitrary to adopt a color based on a second filter that was redder than the filter in question. The choice could just as well have been the shorter wavelength. Or even better, an average "curvature" based on filters passing shorter and longer wavelengths. The adoption of a standard procedure of using the longer wavelength filter only was probably driven by the need to calibrate blue magnitudes, for which shorter filter measurements would be difficult to acquire with good signal-to-noise. (since the blackbody distribution of flux falls off fast on the blue side of the wavelength having maximum flux). Moreover, the various definitions for color are almost always correlated. Thus, for every star in the M67 list if you know B-V it's possible to estimate V-R, and R-I, with fair accuracy.
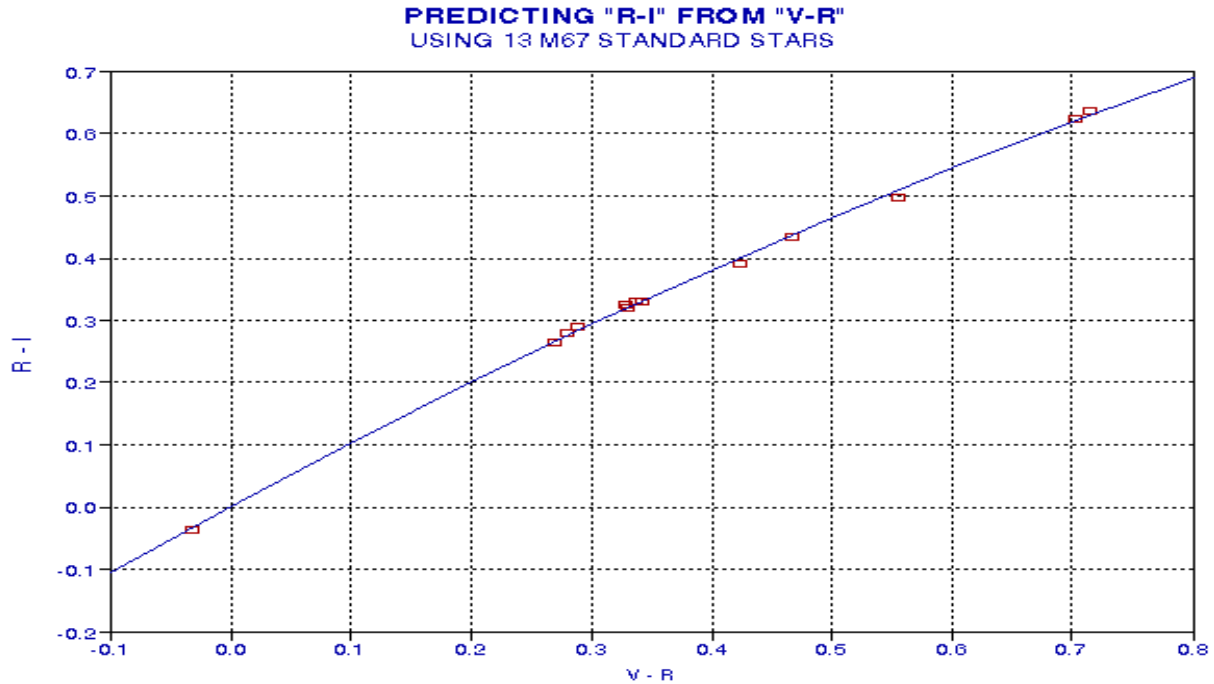
Figure 32 - Correlation of "R-I" with "V-R" for the 13 M67 standard stars.
Residual error of the predicted "R-I" is 0.007 magnitude.

As this plot shows, for "normal" stars if you know one color difference you can predict the other accurately (with a SE of 0.007 magnitudes). Therefore, to the extent that all objects to be dealt with have "normal" blackbody spectra it should acceptable to use "V-I" for correlating "i-I" biases.
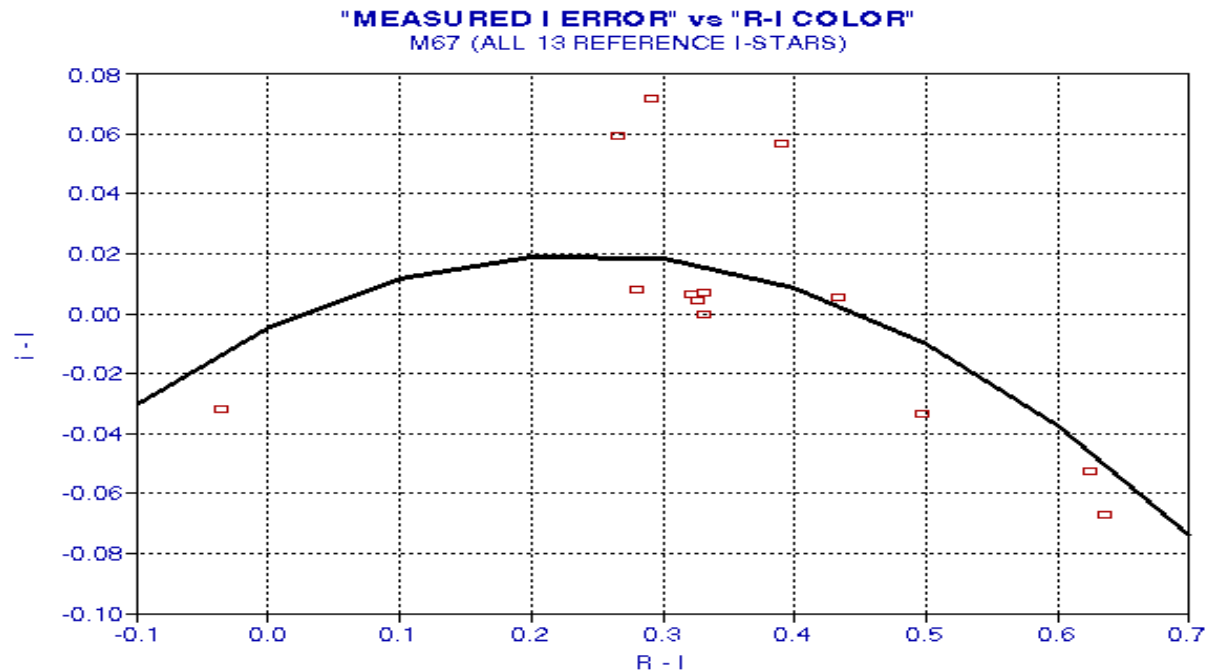
Figure 33 - Correlation of I-magnitude bias "i-I" versus R-I color. The residual of the model fit is 0.026 magnitudes.

As with all 4 previous plots of a bias versus color, the curvature is negative. The stochastic component of uncertainty of these measurements is 0.012 magnitudes, so the scatter off the second-order model fit of 0.026 magnitudes is probably produced by something as systematic as errors in the assumed ("true") I-magnitudes, artifacts in the images used for this analysis, and changes in atmospheric transparency during the observing session. Nevertheless, it is gratifying to know that it may be possible to rely upon this calibration procedure to measure I-magnitudes with an accuracy of 0.026 magnitudes.

Where Things Stand Regarding Alternative Calibration Procedure

It should be acknowledged here that the alternative calibration method suggested in this section can only be used when a large number of comparison stars are available within the CCD image field of view (FOV). This is usually the case for supernova, and might be true for nova. CCD photometry is always easier with a CCD chip affording a large FOV (as with the SBIG ST-8E), and this is especially important when using the alternative calibration procedure. But this may not be the case for all variable stars. If the procedure were to be adopted, it would have this limitation. Nevertheless, provided someone (Arne, for example) goes to the trouble of carefully measuring magnitudes for a large number of stars near new objects of interest, thus creating many nearby comparison stars for that object, the procedure suggested here should be feasible for the rest of the AAVSO CCD membership.

Upon inspecting plots such the pair Fig.'s 26 and 27, there can be little doubt that if one of the comparison stars had been re-assigned to the status of "unknown object" the analysis would have led to a correct magnitude estimate for the object. Even for the blue filter measurements, where departures from the 1:1 line are greater, these differences can be "fit" with a second order equation (as with Fig. 27) with a residual SE of ~0.02 magnitudes.

Additional evaluation of this alternative procedure might require a systematic observing program, with a protocol established by experienced observers.

In the mean time, what is an observer to do who is concerned about the fact that the traditional CCD Transformation Equations are only as valid as the assumption that the air mass and other extinction conditions for the observed object are similar to those that applied when coefficients were determined from the yearly M67 observations? Advances in accuracy might be obtained by making M67 observations at several air masses, leading to coefficient sets that apply to air mass ranges. But even with this additional effort, the seasonal effect caused by vapor burden changes would not be addressed. In theory, the seasonal effect could be assessed by using the other two standard star regions for determining transformation equation coefficients.

The suggestion of this section is that it is not necessary to go to so much work to achieve improved accuracy when a much simpler alternative is available. There may be a fatal flaw in the suggested alternative calibration procedure which escapes this novice eye. Feedback would be appreciated.

Last Update: March 31, 2006